LANDFORMS AND TECTONICS OF THE CENTRAL COAST REGION OF CALIFORNIA

HAMILTON, Douglas H., 2 Bassett Lane, Atherton, CA 94027, dhhgeoconsult@hotmail.com

Abstract

Understanding of the tectonics of the central coastal region of the Southern Coast Ranges of California has been significantly advanced by recent development of two general categories of geoscience knowledge. These are 1.) new developments in landform imaging at regional to detailed local scale, and 2.) imaging of the structure of the underlying crust by seismologic analysis of increasingly well recorded seismicity (eg. Hardebeck 2010) together with acquisition and modeling of gravity and magnetic potential field data (eg. Langenheim et. al. 2012) plus characterization by deep drilling and by geophysical techniques.

The general pattern of contemporary tectonism in the central Coast Ranges and adjacent near coastal offshore is clearly shown by the distribution and form of the principal mountain ranges in the region. Between Monterey Bay and the Transverse Ranges these local ranges mostly have discrete fault-controlled topographic boundaries and overlie zones of concentrated microseismicity. This indicates a characteristic structural form of uplifting "pop-up" wedge blocks for the mountain ranges of the region (as was determined by McLaren et.al., 2008 for the Santa Lucia Range source region of the 2003 San Simeon earthquake). The uplift of the wedge-block ranges represents accommodation to east-west, rotating southward to nearly north-south, regional compression. Earthquakes of M7.0-<7.5 appear possible on the reverse faults along which these ranges are being uplifted.

This general pattern of compressional tectonism onshore is bounded on the west by the 400 km long zone of active strike slip tectonism of the San Gregorio-Hosgri fault system. This system has produced no large earthquake during the 250 years of recorded history but exhibits local paleoseismic evidence of generating earthquakes of M>7.5.

It is suggested here that the evidence from the south central Coast Ranges seen in the terrain as well as in its tectonic underpinning, indicates a level of tectonism and consequent seismic potential that exceeds that now accepted for design and safety analysis of major infrastructure features in the region.

Contents

Synopsis of Poster Concept and Illustrations

The concept that essentially all of the significant terrain features of the study region are expressions of recent and ongoing tectonic deformation, provides the basis for this poster display. Here we show the southern Coast Ranges located athwart the central reach of the San Andreas plate boundary fault and adjacent its west-side branch, the San Gregorio-Hosgri fault zone, to be accommodating extension- induced compression transmitted westward from the Basin and Range province to the east to the Sierra Nevada microplate. From there westward drives this compression structural the crustal shortening between the east margin of the Coast Ranges and the continental slope. Deformation is locally enhanced in the coast and transverse ranges region west of the Garlock fault – San Andreas "Big Bend" juncture in a broad zone extending from the westward bend in the Sierra Nevada Range westward to the continental shelf.

Knowledge of the crustal structure underlying the tectonic terrain of the southern Coast Ranges and surrounding region has recently been advanced by potential field (gravity and magnetic fields) modeling and by plotting the mechanism and "3-D" distribution of well recorded earthquakes ranging from 0 to 6.9 (Loma Prieta) magnitude. Results from these techniques (terrain analysis, potential field modeling, seismology) have been augmented locally by deep drilling, mostly for hydrocarbons, and exploration and research geophysics. The latter techniques have provided much of what is known about faults and other tectonic deformation in the offshore region.

The digital terrain, seismicity, fault mapping, geophysics modeling and offshore geophysics results are shown in the poster figures, and the terrain is further illustrated by a series of Google earth oblique aerial images of prominent uplifts and fault-line scarp hill fronts.

List of Illustrations

Figure No.

6b Digital terrain map showing close correspondence between terrain features and geologically mapped faults, from USGS, 2013

7a Seismicity in the central and southern Coast Ranges and adjacent offshore, recorded since 1980 based on relocations by Waldhauser and Schaff (2008) north of 36ºN and by Hardebeck (2010) south of 36ºN. Inset plot shows seismicity in the south-central Santa Lucia Range through early December 2003, prior to the 2003 M6.5 San Simeon earthquake. Locations of seismicity hypocenter cross sections are shown on this plot and are identified as to section designation on Figure 10b.

7b Seismicity as on Figure 7a, with selected epicenters color coded to indicate focal mechanism. Seismicity plot provided by Hardebeck (2013).

8 Seismicity prior to late December 2003 in the south central Coast Ranges and adjacent continental shelf, with digital terrain base of the onshore region. Note the close correspondence of most seismicity with the uplifted tectonic terrain of the Santa Lucia Range, Irish Hills of the San Luis Range, and Casmalia-Soloman Hills – from NCEDC, 2006, plotted by UNR Seismological Labl 2006.

9 Earthquake focal mechanisms, southern Coast Ranges, western Transverse Ranges and adjacent offshore region, from McLaren et al., 2008 and Hardebeck, 2010

10a Seismicity in the central and southern Coast Ranges and adjacent offshore, recorded since 1980 based on relocations by Waldhauser and Schaff (2008) north of 36ºN and by Hardebeck (2010) south of 36ºN. Inset plot shows seismicity in the south-central Santa Lucia Range through early December 2003, prior to the 2003 M6.5 San Simeon earthquake. Locations of seismicity hypocenter cross sections are shown on this plot and are identified as to section designation on Figure 10b.

10b Digital terrain image of the central and southern Coast Ranges and western extent of the western Transverse Ranges. The traces of offshore reaches of the San Gregorio Hosgri fault zone are based on seismic reflection geophysical data. The trace of the offshore Shoreline fault is based on the alignment of small earthquakes along it and south of Point Buchon, on its sea floor terrain expression as seen on Multibeam sea floor imagery. Locations of seismicity cross

Notes on Tectonic Terrain Features as imaged on Figures 2, 4, 5 and 6b and annotated on Figure 3

1. Dome or welt like terrain of the Santa Cruz Mountains and Gabilan Range, each along the west side of the San Andreas fault. Although containing faults in their roots which are probably related to the adjacent San Andreas, neither of these mountain ranges are uplifting wedge blocks.

2. East margin of the Coast Ranges, fronting the Central Valley. Southward from the vicinity of Altamont Pass to near Coalinga this terrain feature is sharply defined and represents the fault-line scarp resulting from underthrusting of the Coast Ranges by the western margin of the Sierra Nevada basement block or "microplate". Local reaches of this contact are mapped as the San Joaquin fault. From the vicinity of Coalinga nearly to the south end of the Central Valley the Coast Ranges-Central Valley boundary is not sharply defined and is featured by a series of topographically expressed anticlinal folds in the valley floor adjacent to the high-standing Temblor Range situated between the valley and the San Andreas fault.

3. The south end of the Central Valley terminates abruptly at the Tehachapi mountain range. The valley margin of this range cross structure is sharply defined and corresponds to the fault-line scarps of the south-dipping Wheeler Ridge and White Wolf faults.

4. The northern Santa Lucia Range is bounded by high oversteepended margins that clearly appear as fault-line scarp terrain features. Potential field modeling across the Sierra de Salinas escarpment fronting the Salinas Valley on the east and the seaward-facing escarpment on the west, together with a well defined eastward dipping pattern of earthquake hypocenters beneath the west-side escarpment demonstrate that the northerly part of the range is a "popup" wedge block, that is being compressionally uplifted between range-margin inward dipping reverse faults.

5. South of the Sierra de Salinas escarpment the east margin of the Santa Lucia Range becomes lower and less sharply defined and bulges into the adjacent Salinas Valley. The interior of this "bulge" is marked by a narrow linear rift which is the surface expression of the strike slip Rinconada fault. The east facing valley margin of the terrain bulge, which closes off the wide trough of the Salinas Valley to the north, appears to correspond to the Los Lobos thrust. This structure is known in the subsurface from oil well intercepts in the nearby San Ardo oil field. Note that the area of this oil field lies within a local concentration of seismicity (e.g., Figures 8 and 10a, seismicity cross section E-E' of Figure 12). The seismicity hypocenters are clustered between 3 and 12 km depth, in crystalline basement below the depth of oil field activity and do not occur in a pattern suggestive of any particular structure. It seems possible, however, that in the San Ardo area the seismicity may be related to load removal stress changes within the seismogenic level of the crust, associated with extraction of very large amounts of oil and water from the overlying near-surface oil field.

6. The southernmost part of the southern Coast Ranges is featured by a series of arcuate local ranges all of which display steep erosionally dissected southwest-facing escarpment slopes and gradual downward ramping northeast slopes. The most prominent of these terrain features are the La Panza and

Morales Ranges which are fronted on the southwest by faults of the same name. A lower range front follows the trace of the southernmost reach of the Rinconada fault.

7. Oceanic - San Andreas lineament. The La Panza and Morales fault line escarpments form the southeasterly reach of a prominent terrain lineament that aligns with the San Andreas fault south of its "Big Bend" and continues northwestward as a well marked terrain feature following the Oceanic fault to its juncture with the San Simeon fault on the coast. We here refer to this feature as the Oceanic – San Andreas lineament. The lineament forms a boundary between the characteristic terrain of separate ranges and intervening basins of the southern Coast Ranges to the north and the generally mountainous terrain of the western Transverse Ranges that exists between the Cuyama Valley and the Santa Barbara channel. The terrain aspect of the lineament feature is suggestive of it being a coherent tectonic dislocation with its terrain defined by the south ends of the en echelon series of active reverse (or right reverse) faults along its northeast side. The terrain relationship of the series of northwest trending ranges to the Oceanic-San Andreas lineament could be interpreted as indicating branching and possibly transmission of some right slip from the San Andreas fault south of its "Big Bend" abrupt turn from west-northwest to northwest strike, into the reverse faults. It may also be noteworthy that the obvious compressional deformation indicated by the series of reverse faults extending from the lineament into the southern Coast Ranges is within the zone of enhanced compression that extends west-southwest from the terrain-indicated enhanced extension along the southwest margin of the Basin and Ranges tectonic province located east of the "Big Bend".

8. Wedge-block popup uplifts of the westernmost western Transverse Ranges and southwesternmost southern Coast Ranges. As shown on Figure 3 there are two prominent tectonic terrains in the subject region that geologic, geophysical, and seismicity data confirm as being "popup" structures. These are the Irish Hills and their southeasterly continuation the San Luis Range, and the Casmalia-Soloman Hills uplift. Each of these features as well as the southern Santa Lucia Range to the north, are uplifting along paired downward converging reverse faults. The down dip configuration of these faults in each case involves a "master" fault beneath the higher and steeper southwest facing range front and a back thrust that dips towards and intersects the "master" thrust. All of these reverse or thrust faults and their intervening popup wedge uplifts continue along strike to intersect the San Simeon-Hosgri reach of the San Gregorio-Hosgri fault at angles of 25 to 35 degrees. For the Irish Hills, the southwest-side "master" thrust partly impinges on the vertical strike-slip Shoreline fault splay of the San Simeon-Hosgri in the subsurface although this fault is exposed at the surface along the base of the San Luis Range to the southeast. All of these faults display active seismicity and/or clear evidence of late Quaternary surface displacement.

9. Zone of crustal extension in the southwestern Basin and Range culminating at the eastern frontal faulting of the Sierra Nevada, with crustal shortening continuing west-southwest along the trend of this zone into the continental shelf. The major components of this roughly 150 km wide zone are readily discernable in the terrain, beginning on the east with the southward widening of intramontane troughs in the southwesternmost section of the Basin and Ranges, continuing to the west as the pronounced bend in the Sierra Nevada Range

and the "Big Bend" deflection of the San Andreas fault and development of the thrust dominated terrain extending to the shoreline. The westernmost extent of this apparently extension driven compression is seen in the sea floor deformation by north-northwest oriented thrust faults in the continental shelf west of the shoreline between Point Conception and Point Sal.

10. The south end of the Sierra Nevada Range bends to the west in a broad arc extending some 140 km north from its southern termination as the Tehachapi Range along the Garlock fault. This bend is directly opposite the area of apparently enhanced crustal extension in the southwestern corner of the Basin and Range to the east.

11. The convex to the west arcuate uplift along the west margin of the bend in the Sierra Nevada Range. This uplift, referred to generally as Round Mountain and the setting for several oil fields, is unique to the west margin of the Sierra and has a terrain aspect typical of the domal upwarp over active thrust faults. The well studied structure of the 1000 m. thickness of Tertiary strata that underlie the Round Mountain surface, however consists of a complex of normal faults. Given this apparent paradox, we here suggest that the Round Mountain terrain is in fact the terrain expression of an underlying thrust but that the normal faults in the overlying section result from local domal extension in the thrust upper plate. The Round Mountain thrust as hypothesized would then occupy the same local compressional environment as the Plieto and Wheeler Ridge thrust faults at the south end of the San Joaquin Valley and the Elk Hills and related compressional terrain features along the valley margin to the west.

12. The "Big Bend" of the San Andreas fault. Here the alignment of the clearly expressed rift terrain of the San Andreas fault bends gradually more westerly northward from N64W to the south to N77W in the bend, then more abruptly to N40W continuing northward in the southern Coast Ranges. Kinematically this bend and realignment appears to mainly represent geometric accommodation to west-southwestward movement of the crust located north of the Garlock fault and internally within this crustal plate, the left-reverse White Wolf fault. However the terrain of the bend also appears to reflect the southward movement of the Central Valley – Sierra Nevada crustal plate with resultant compressional impingement on the central part of the western Transverse Ranges. Terrain features in the "Big Bend" area include the Plieto/Wheeler Ridge thrust uplift located directly north of the bend and compressional features represented by fold-belt hills and fault scarps located both east and west of the San Andreas rift north of the bend area. The highest points in the main body the western transverse Ranges, Mt. Pinos and Frazier Mountain, are located immediately south of the Big Bend.

13. Active fold and thrust belt in the southern part of the offshore Santa Maria Basin. This local zone of crustal shortening deformation is located west of the southernmost reach of the Hosgri. The trend of fold axes and strike of faults in this zone is north-northwest which is parallel to the adjacent reach of the Hosgri but at an angle of 40 to 60 degrees to the onshore structures in the east block of the Hosgri and westernmost part of the western Transverse Ranges. The east northeast – west-southwest crustal shortening in the local zone of deformation however, is directly in line and orientation to be responding to compression from the Big Bend deflection to the east.

14. Local seismicity zone, in the continental shelf centered approximately 40 km offshore from the coastline between point Sal and Purisima Point (Figure 8). As shown on Figure 9 most of the earthquakes in this zone have reverse/thrust mechanisms with orientation indicating east-northeast – west-southwest compression. This local seismicity zone originates in a fold and thrust belt that is located in the outer margin of the offshore Santa Maria Basin and like the item 13 zone is oriented so as to respond to compression along the trend extending through the San Andreas "Big Bend".

15. The Murray fracture zone – Anacapa - Dume thrust – Santa Maria and San Gabriel south frontal faults lineament

This lineament consists of three aligned terrain structural features. On the west, extending from an apparent easterly termination at the base of the continental slope, more than 2000 km across the floor of the Pacific Ocean is the apparently extinct but still visible in the sea floor terrain Murray fracture zone transform fault. In direct line with this feature is the east-west aligned terrain boundary between the sea floor shelf of the Santa Barbara basin and channel islands and the basin and range-like terrain of north-northwest aligned submarine ridges and troughs of the Southern California Borderland. This boundary has been interpreted as the escarpment of a north-dipping "Anacapa-Dume thrust". This thrust zone extends onshore as the series of separately named faults that form the overthrust boundary between the south-thrusting Santa Monica and San Gabriel mountains and the Los Angeles – San Bernardino basin. These features are all prominent components of the overall terrain lineament forming the south boundary of the western Transverse Ranges.

Proposed Kinematic Neotectonic Model

A generalized proposed terrain-based kinematic neotectonic model of the region extending from the continental shelf offshore from the southern Coast Ranges and western Transverse Ranges to the southwestern corner of the Basin and Range province is shown on Figure 26. This model involves relative movements among and stress-strain relationships between, nine crustal blocks. Boundary structures within the model region comprise the Garlock, San Andreas, and San Gregorio-Hosgri predominantly strike slip faults and the southern Coast Ranges coast frontal and Anacapa-Dume thrust faults. The boundary between the southern Coast Ranges and western Transverse Ranges blocks, as interpreted and referred to herein as the "Oceanic – San Andreas lineament" consists of possibly linked segments of several thrust faults and one strike slip (the southern Rinconada) fault.

Relative movement between blocks in the model region is centered around the local west-southwestward deflection of the south to south eastward movement of the crustal blocks on the northeast side of the San Andreas fault. This deflection is concentrated along, and generally east and west of the 60 km reach of the San Andreas north of the intersection with it of the Garlock fault. Resulting deformation in the area of this deflection includes development of the north vergent Wheeler Ridge and Plieto thrusts at the south end of the Central Valley north of this intersection, and of the greatest uplift of the central western Transverse Range, southwest of the intersection.

The westward deflection must also contribute to the left slip along east-west aligned faults and compressional crustal shortening in the westernmost part of the western Transverse Ranges. However the overall pattern of left slip on east-west aligned faults in the western Transverse Ranges continues to the south frontal thrust south boundary of this block. This pattern may represent internal shearing of the western Transverse ranges block as it is extruded westward by it collision with the Peninsular Ranges and southern California offshore borderland block moving northward into the gradual west bend of the San Andreas south of its "Big Bend" deflection.

Compression related to the "Big Bend" deflection also appears to be transmitted across the southernmost reach of the Hosgri fault to create the local active fold and thrust belt of deformation in the southernmost part of the offshore Santa Maria Basin.

Both the San Andreas and San Gregorio-Hosgri faults are steep, mostly vertical strike slip block boundary faults but only the San Andreas continues both north and south of the region of this tectonic model. The San Gregorio-Hosgri is the only west side splay of the San Andreas north of its San Jacinto splay in Cajon Pass. But like the San Andreas the San Gregorio fault has several important east side splays including (probably) the Monterey Bay fault zone, several large faults extending southward into the Santa Lucia Range, and the Shoreline fault along the southwest margin of the Irish Hills. Reverse faults that intersect and terminate at the San Simeon-Hosgri reach of the San Gregorio-Hosgri consist of the Arroyo Laguna-Oceanic, the San Luis Range and Los Osos, and the Lions Head and Casmalia faults. The Hosgri fault dies out southward in a complex of folds and reverse faults offshore from the Santa Ynez Valley. The neotectonic structure and terrain of the interiors of the both the southern Coast Ranges block and the westernmost part of the western Transverse Ranges consists of a series of wedge-block uplifts bounded by downward converging thrust faults (typically a primary thrust and a large back thrust pair) with several of the thrust or reverse faults transitioning southward to strike slip. The Reliz and Oceanic reverse faults to Rinconada and West Hausna strike slip faults are the most prominent examples of such a transition. The neotectonic model presented here suggests that the right slip on faults of the southernmost southern Coast Ranges may splay northward from the "Oceanic-San Andreas lineament", which is positioned to convey right slip into this region from a direct connection with the "Big Bend" reach of the San Andreas.

The general east-northeast - west-southwest crustal shortening in the coastal side of the southern Coast Ranges block and west end of the western Transverse Ranges block occurs in response to compression from the Basin and Ranges westward extension rather from some effect of the boundary strike slip faults except in the San Andreas "Big Bend" region, where the westward movement from the Basin and Ranges extension deflects the San Andreas to a left bend with resultant local compression and deformation. The model described here has developed during latest Neogene time and its structural features and their expression in the terrain are the result of on-going tectonic activity. This is shown both by the youthful terrain and by pervasive seismicity seen in the brief historic record and in paleoseismic studies of tectonic structures that have not had associated historic seismicity.

Selected References and Data Sources

Alterman, Ina B., Richland B. McMullen, Lloyd S. Cluff, and D. Burton Slemmons. (Eds.), 1994, Seismotectonics of the Central California Coast Ranges, Geol. Soc. Amer. Spec. Paper 292

Clark, D.H., Hamilton, D.H., Hall, N.T., and Heck, R.G., 1987, Timing and style of Neogene deformation within the offshore Santa Maria Basin, California (abs.): EOS, v. 68, no. 44, p. 1365

Compton, R.R., 1966, Analyses of Pliocene-Pleistocene deformation and stresses in the northern Santa Lucia Range, California: Geological Society of America Bulletin, v. 77, p. 1361-1380.

Crouch, J., Bachman, S.B., and Shay J.T., 1984, Post-Miocene compressional tectonics along the central California margin: in Crouch, J., and Bachman, S.B., eds., Tectonics and sedimentation along the California margin; Pacific Section, S.E.P.M., v. 38, p. 37-54.

Dibblee, T.W., Jr., 1974, Geologic map of the San Luis Obispo 15-minute quadrangle, California: U.S. Geological Survey Open-File Map, scale 1:62,500.

Dickinson, W.R., Mihai Ducea, Lewis I. Rosenberg, H. Gary Greene, Stephan A. Graham, Joseph E. Clark, Gerald E. Weber, Steven Kidder, W. Gary Ernest, and Earl E. Brabb, 2005, Net Dextral slip, Neogene San Gregorio-Hosgri Fault Zone, Coastal California: Geologic Evidence and Tectonic Implications, Geol. Soc. Amer. Spec. Paper 391, 43 p.

Google Earth, 2012, Oblique aerial images of tectonic terrain features, central and southern Coast Ranges, California.

Goter, Susan K., Gail P. Thelen, and Richard J. Pike, 1992, Earthquakes in the Conterminous United States, (1534-1991), USGS open-file Report 92-327.

Hamilton, D.H., 2012, Irish Hills/San Luis Range Tectonics and Fault Model, PG&E SSHAC Workshop, 2 November, 2012.

Hamilton, D.H., 1984, The tectonic boundary of coastal central California: unpublished Ph D. thesis, Stanford University, California, 290 p.

Hardebeck, Jeanne L. 2013, Geometry and Earthquake Potential of the Shoreline Fault, Central California, Bull Seismol. Soc. Amer., Vol 103, No. 1 pp 447-462, Feb. 2013, doi; 10.1785/012012075

Hardebeck, J.L., (2010), Seismotectonics and fault structure of the California central coast, Bull. Seismol. Soc. Am. 100, 1031-1050 (earthquakes south of 36º N).

Hill, D.P., Eaton, J.P., and Jones, L.M, 1990, Seismicity, 1980-86, in Wallace, R.G., Ed. The San Andreas Fault system, California, U.S.G.S. Prof. Paper 1515, 1990.

Hoskins, E.G. and Griffiths, J.R., 1971, Hydrocarbon potential of northern and central California offshore: in Cram, I.H., ed., Future petroleum provinces of the United States – their geology and potential: American

Association of Petroleum Geologists Memoir 15, p. 212-228.

Jennings, Charles W. William A. Bryant, and George Saucedo, 2010, Fault Activity Map of California, California Geologic Data Map Series, Map No. 6, California Geological Survey.

Johnson, Samuel Y. and Janet T. Watt, 2012, Influence of fault trend, bends, and convergence on shallow structure and geomorphology of the Hosgri strike-slip fault, offshore central California, Geosphere; Dec. 2012, v. 8; no. 6; p1632-1656; doi: 10.1130/GES00830.1; 20 figures

Langenheim, V.E., R.C. Jachens, R.W. Graymer, J.P. Colgan, C.M. Westworth, and R.G. Stanley, 2012, Fault geometry and cumulative offsets in the central coast Coast Ranges, California: Evidence for northward increasing slip along the San Gregorio-San Simeon-Hosgri fault, Lithosphere, www.gsapubs.org doi: 10.1130/L233/

Leslie, R.B., 1981, Continuity and tectonic implications of the San Simeon - Hosgri fault zone, central California: U.S. Geological Survey Open-File Report 81-430, 59 p.

McCulloch, D.S., 1989a, Evolution of the offshore central California margin, in Winterer, E.L., Hussong, D.M., and Deeker, R.W., eds., The eastern Pacific Ocean and Hawaii: Boulder, Geological Society of America, Geology of North America, v. No. p. 439-470.

McLaren, M.K., Hardebeck, J.L., VanderElst, N., Unruh, J.R., Bawden, G.W., and Blair, J.L., 2008, Complex Faulting Associated with the 22 December 2003 Mw6.5 San Simeon, California, Earthquake, Aftershocks and Post Seismic Surface Deformation, Bull. Seismol. Soc. Am., v. 98, No. 4, pp 1659-1680.

McLaren, M.K., and W.U. Savage (2001). Seismicity of south-central coastal California: October 1987 through January 1997, Bull. Seismol. Soc. Am. 91, 1629-1658.

Mount, V.S. and Suppe, J, 1992, Present-Day Stress Orientations Adjacent to Active Strike slip Faults: California and Sumatra, Journal of Geophysical Research, Vol. 97 No. B8 pp. 11995-12013.

Northern California Earthquake Data Center (NCEDC), 2008. Epicenters and hypocenters of earthquakes recorded between 1988 and April 2008.

Namson, J., and Davis, T.L., 1990, Late Cenozoic fold and thrust belt of the Southern Coast Ranges and Santa Maria Basin, Assoc. Pet. Geol. Bull, v. 74, pp. 467-491.

Nitchman, S.P., 1988, Tectonic geomorphology and neotectonics of the San Luis Range, San Luis Obispo County, California: University of Nevada, Reno, M.S., thesis, 120 p.

_______________, and Slemmons, D.B., 1994, The Wilmar Avenue Fault: A Late Quaternary Reverse Fault Near Pismo Beach, California, Coast Ranges, Geol. Soc. Am Special Paper, I.B., Alterman, R.B., McMullen, L.S., Cluff, and D.B., Slemmons, (Editors) Vol. 292, 103-110.

Pacific Gas and Electric Company, 1988, Long Term Seismic Program, Final Report to U.S. Nuclear Regulatory Commission for Diablo Canyon Power Plant, Docket Nos. 50-275 and 50-323.

_______________, 1974, Geology of the southern Coast Ranges and the adjoining offshore continental margin of California, with special reference to the geology in the vicinity of the San Luis Range and Estero Bay: Appendix 2.5D, FSAR, Diablo Canyon Nuclear Power Plant, AEC Docket Nos. 50-275 and 50-323. (Prepared by Earth Sciences Associates, Inc.).

Page, B.M., 1981, The southern Coast Ranges, in Ernst, W.G., ed., The geotectonic development of California (Rubey Volume I) Englewood Cliffs, New Jersey, Prentice-Hall, p. 329-417.

Page, B.M., Wagner, H.C. McCulloch, D.S., Silver, E.A., and Spotts, J.H., 1979, Geologic cross section of the continental margin off San Luis Obispo, southern Coast Ranges, and the San Joaquin Valley, California: Geological Society of America Map and Chart Series, MC-28G, 12 p., 1 map, scale 1:250,000.

Richardson, H.W., 1923, Shoreline Physiographic of the Santa Lucia Mountains unpub MS thesis Stanford University

Taliaferro, N.L., 1943, Geologic history and structure of the central Coast Ranges, California: California Division of Mines and Geology Bulletin 118, p. 119-163.

Thelin, Gail P. and Richard J. Pike, 1991, Landforms of the Conterminous United Sates, A Digital Shaded-Relief Portrayal, USGS Misc. Inv. Series Map I-2206

Unruh, J.R., 1991, Uplift of the Sierra Nevada and implications for late Cenozoic epeirogeny in the western Cordillera, Geological Society of America Bulletin, v. 103, p. 1395-1404.

Unruh, J.R., Humphrey, J. and Barron, A., 2003, Transtensional model for the Sierra Nevada frontal fault system eastern California: Geology, v.31, no. 4, p. 327-330

U.S. Geological Survey, 2013, Digital Terrain Image

Wakabayashi, J. and Sawyer, T.L. , 2001, Stream incision, tectonics, uplift and evolution of topography of the Sierra Nevada, California: Journal of Geology, v. 109, p. 539-562.

Waldhauser, F., and D.P. Schaff (2008), Large-scale relocation of Northern California seismicity using cross-correlation and double difference methods J. Geophys. Res., 113, B08311, doi: 10.1029/2007JB005479 (earthquakes north of 36ºN)

Zoback, M.L. 1989. State of stress and modern deformation of the northern Basin and Range Province J. Geophys. Res. 94, 7105-7128

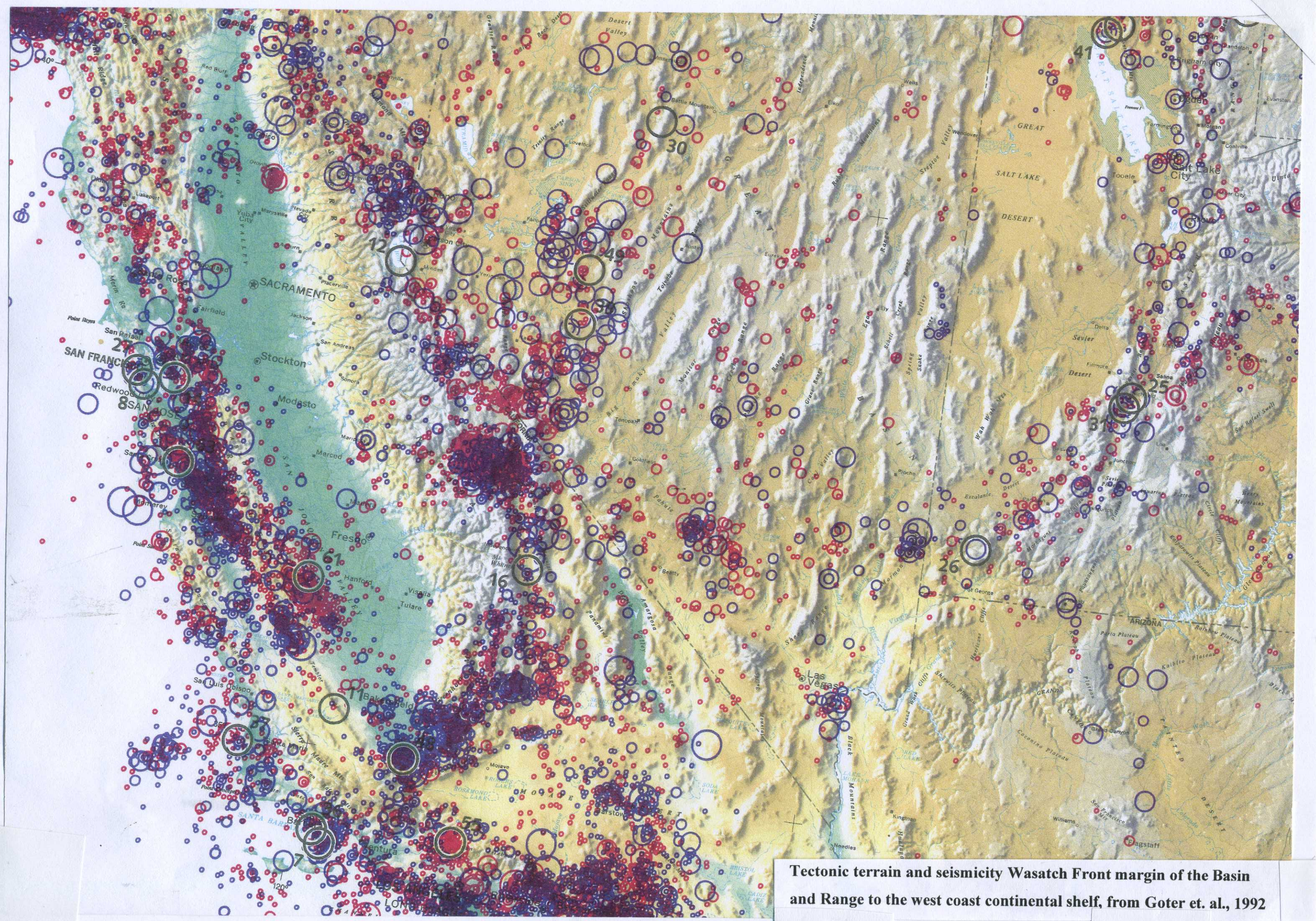

Tectonic terrain and seismicity Wasatch Front margin of the Basin and Range to the west coast continental shelf, from Goter et. al., 1992

Figure 1

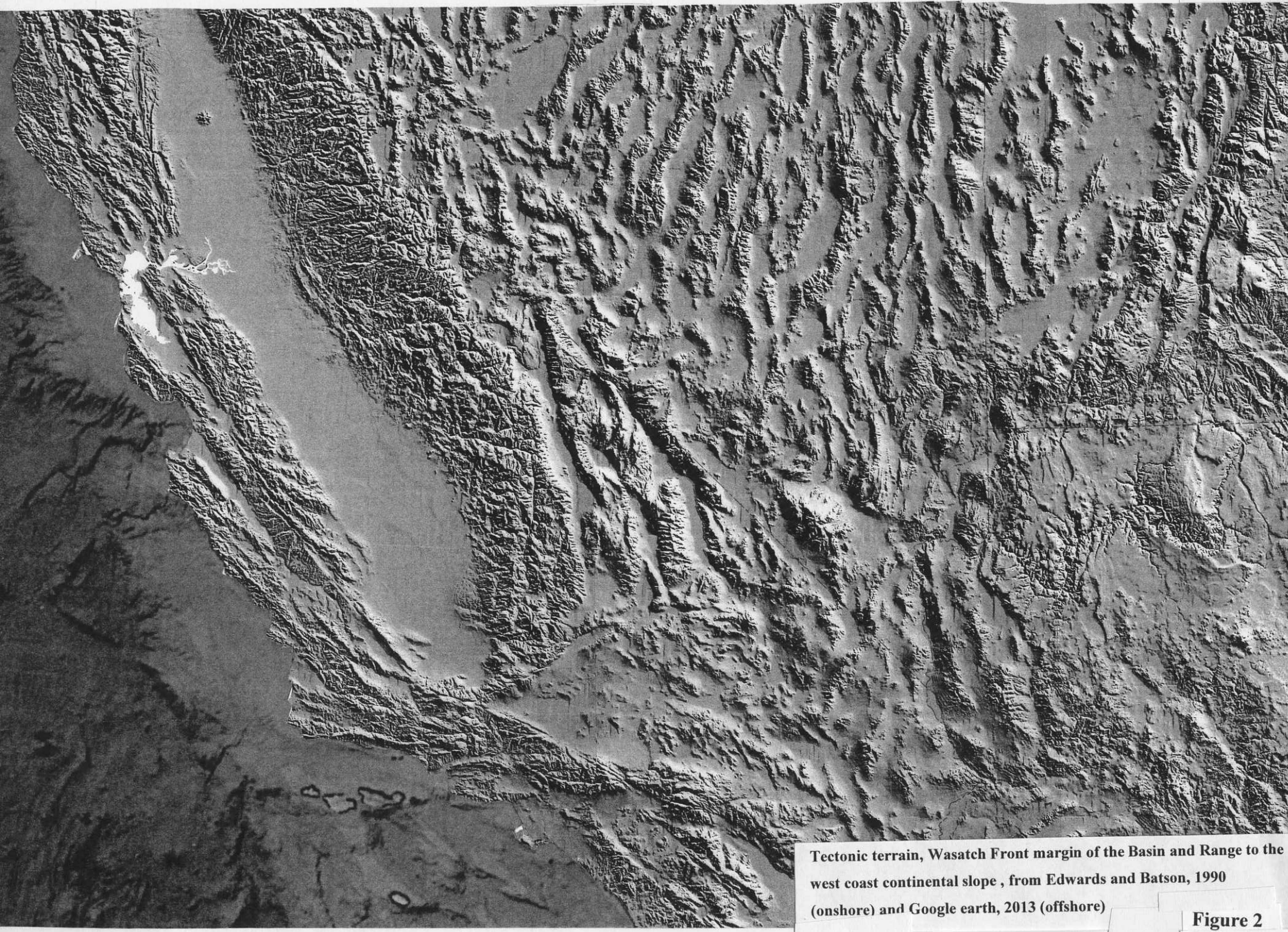

Tectonic terrain, Wasatch Front margin of the Basin and Range to the west coast continental slope , from Edwards and Batson, 1990 (onshore) and Google earth, 2013 (offshore)

Figure 2

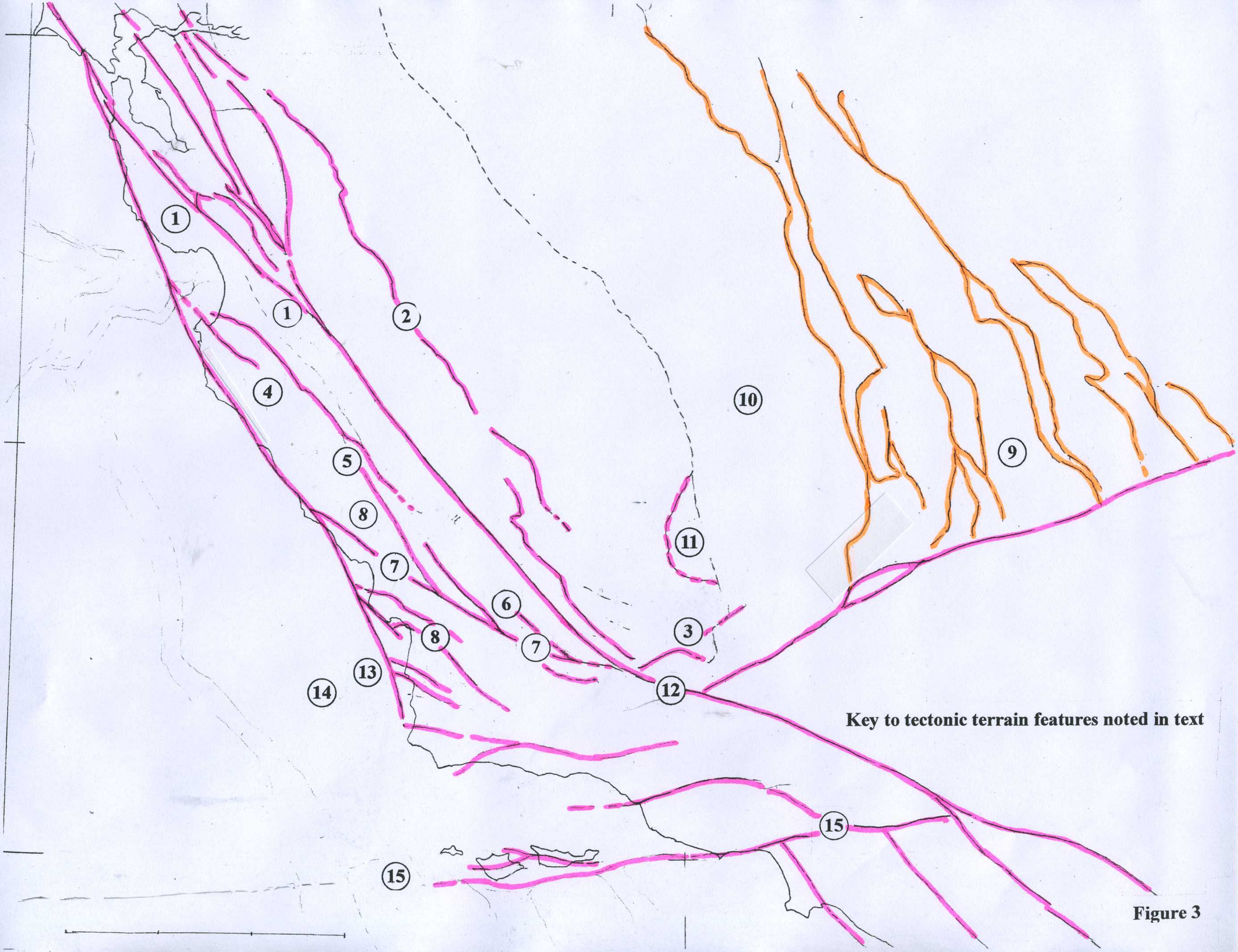

Key to tectonic terrain features noted in text

Figure 3

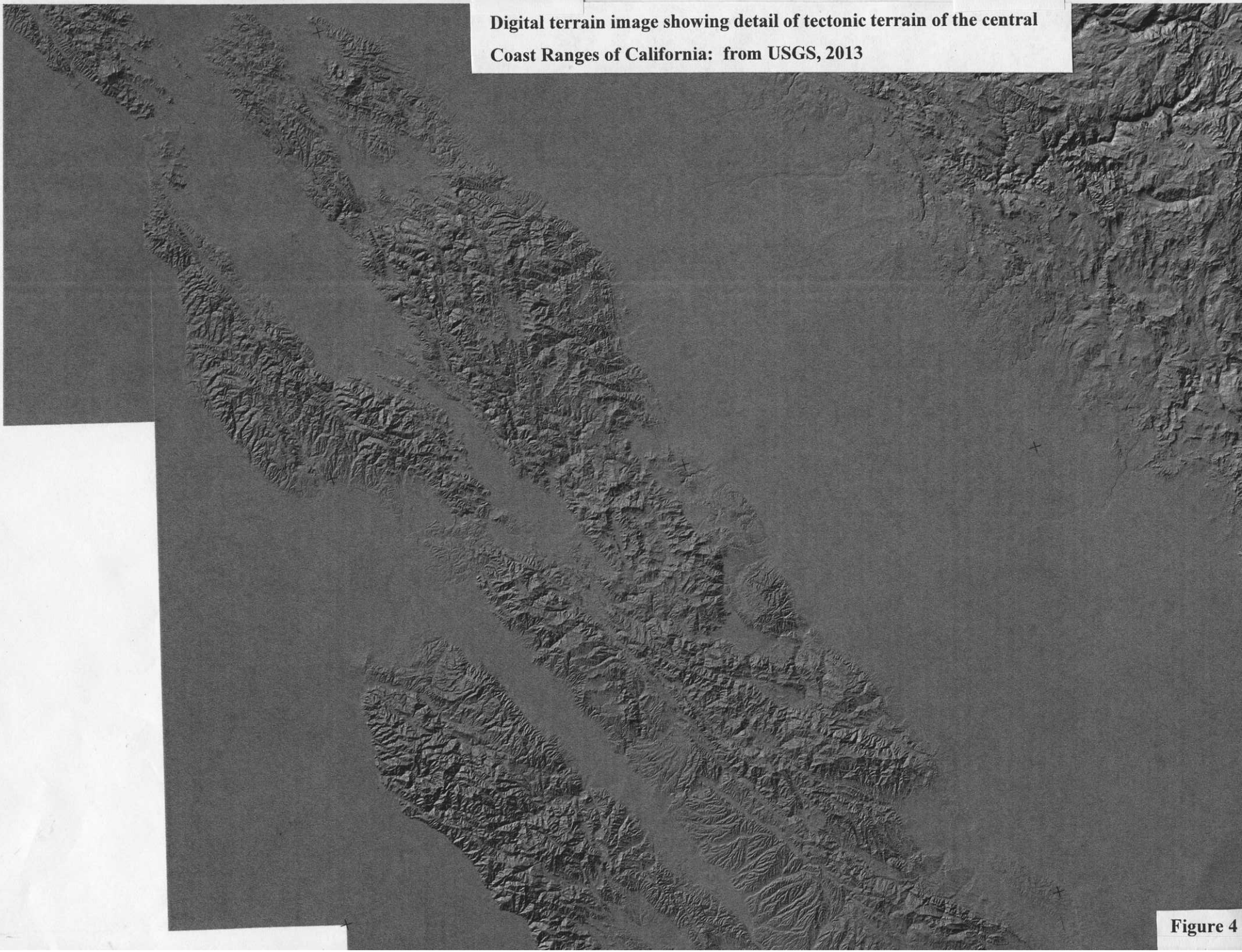

Digital terrain image showing detail of tectonic terrain of the central Coast Ranges of California: from USGS, 2013

Figure 4

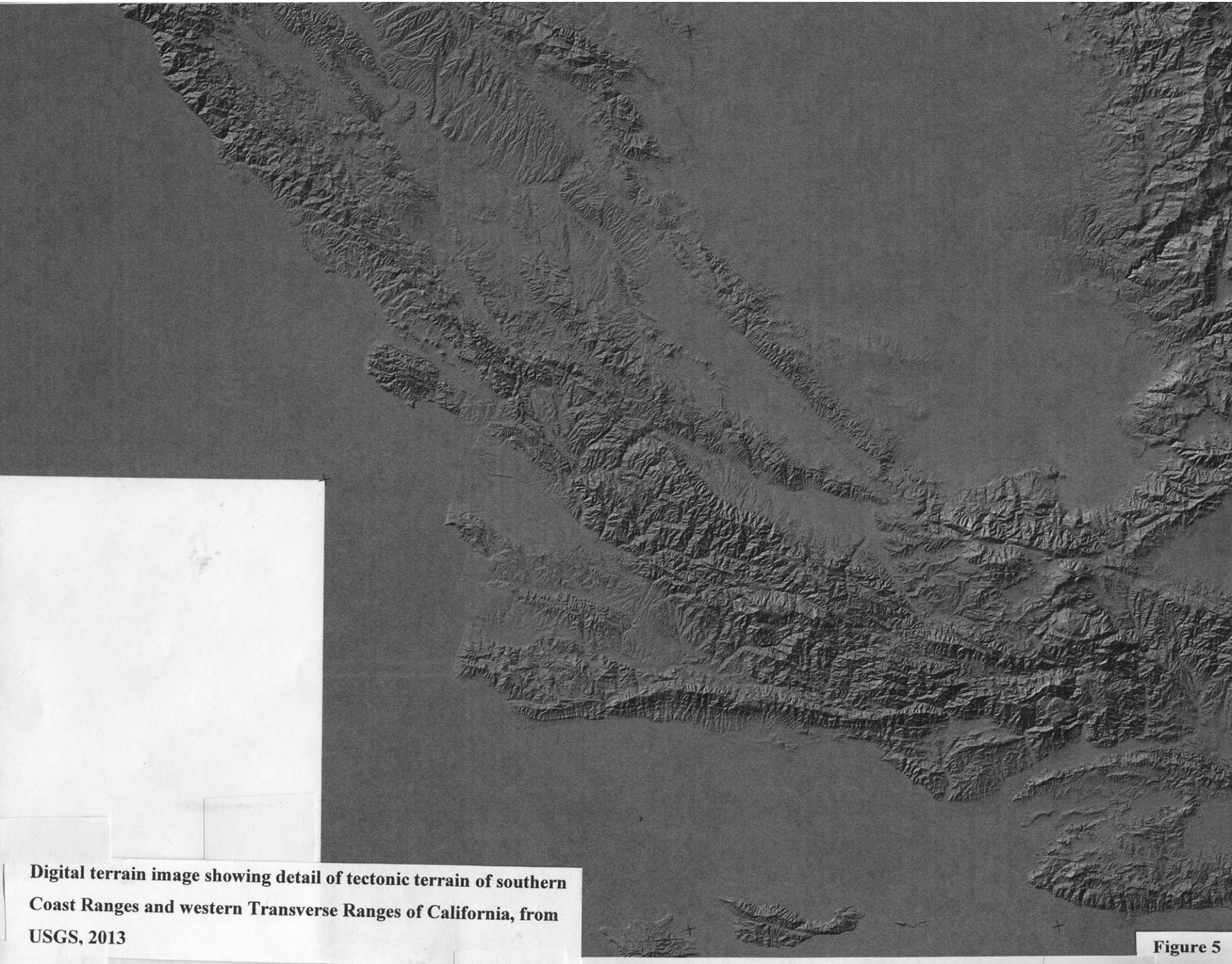

Digital terrain image showing detail of tectonic terrain of southern Coast Ranges and western Transverse Ranges of California, from USGS, 2013

Figure 5

Fault map of the southern Coast Ranges and western Transverse Ranges of California from Jennings et. al. 2010

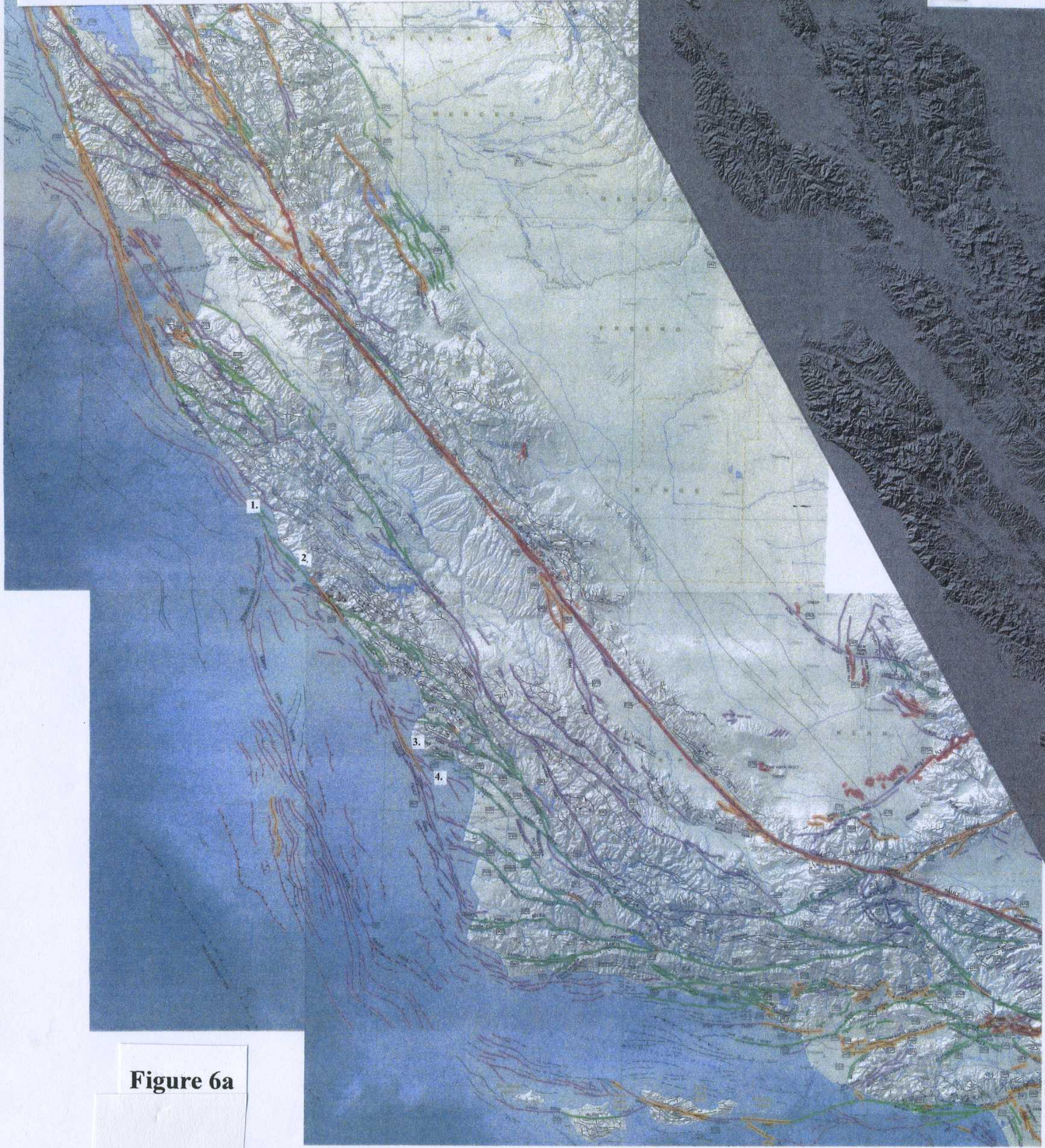

Figure 6a

Digital terrain map showing close correspondence between terrain features and geologically mapped faults, from USGS, 2013

Figure 6b

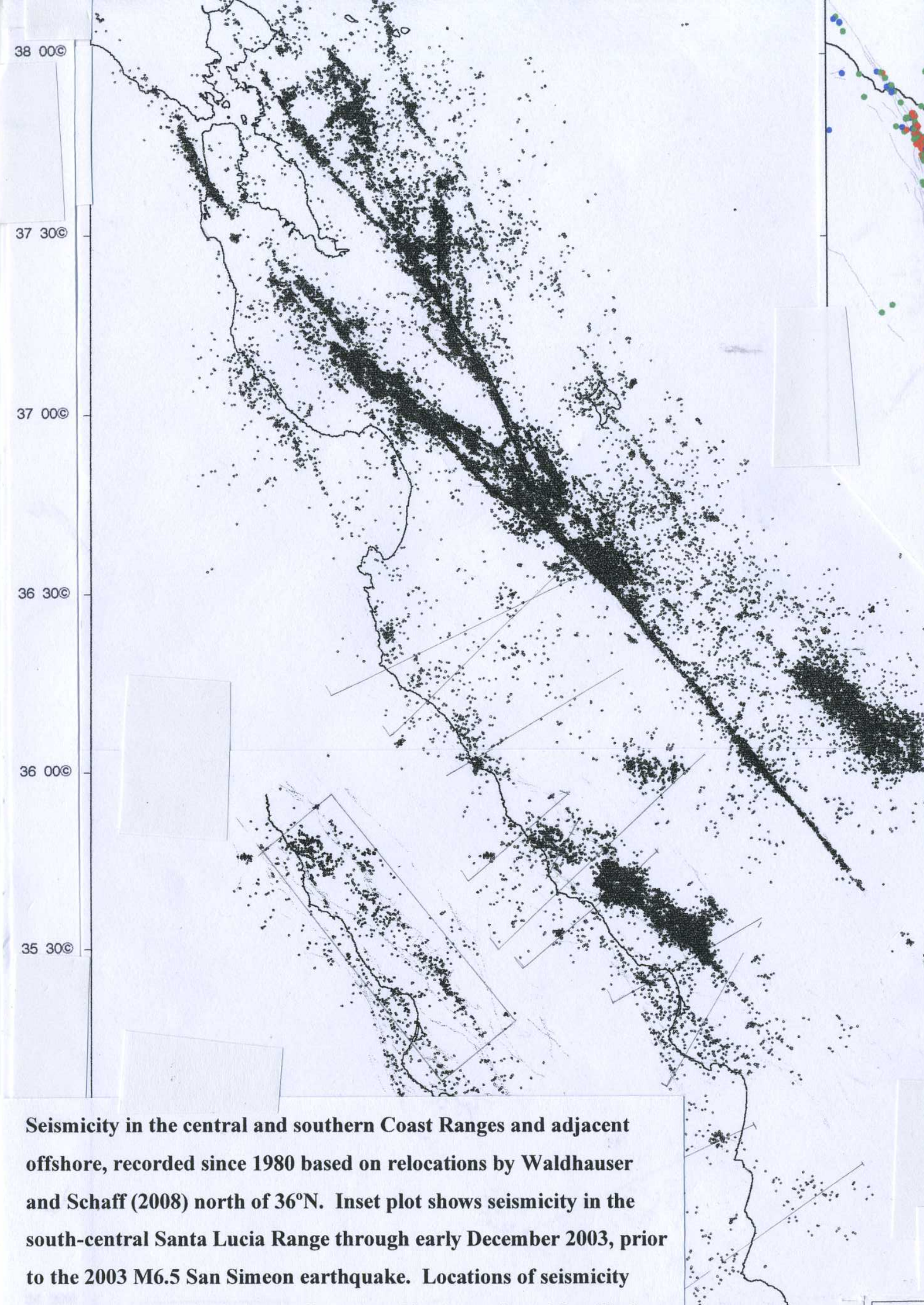

Seismicity in the central and southern Coast Ranges and adjacent offshore, recorded since 1980 based on relocations by Waldhauser and Schaff (2008) north of 36°N. Inset plot shows seismicity in the south-central Santa Lucia Range through early December 2003, prior to the 2003 M6.5 San Simeon earthquake. Locations of seismicity hypocenter cross sections are shown on this plot and are identified as to section designation on Figure 10.

Figure 7a

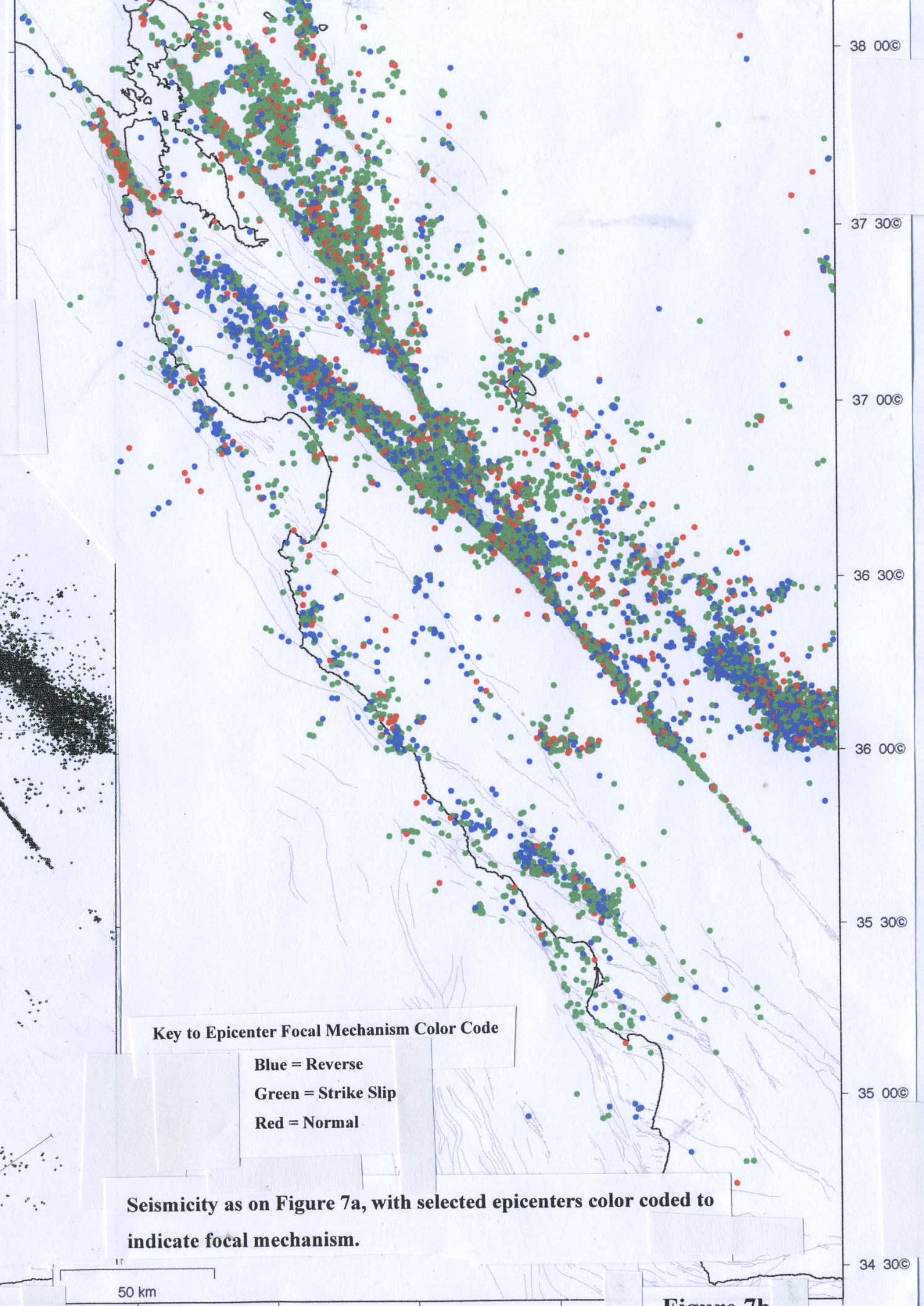

Seismicity as on Figure 7a, with selected epicenters color coded to indicate focal mechanism.

Figure 7b

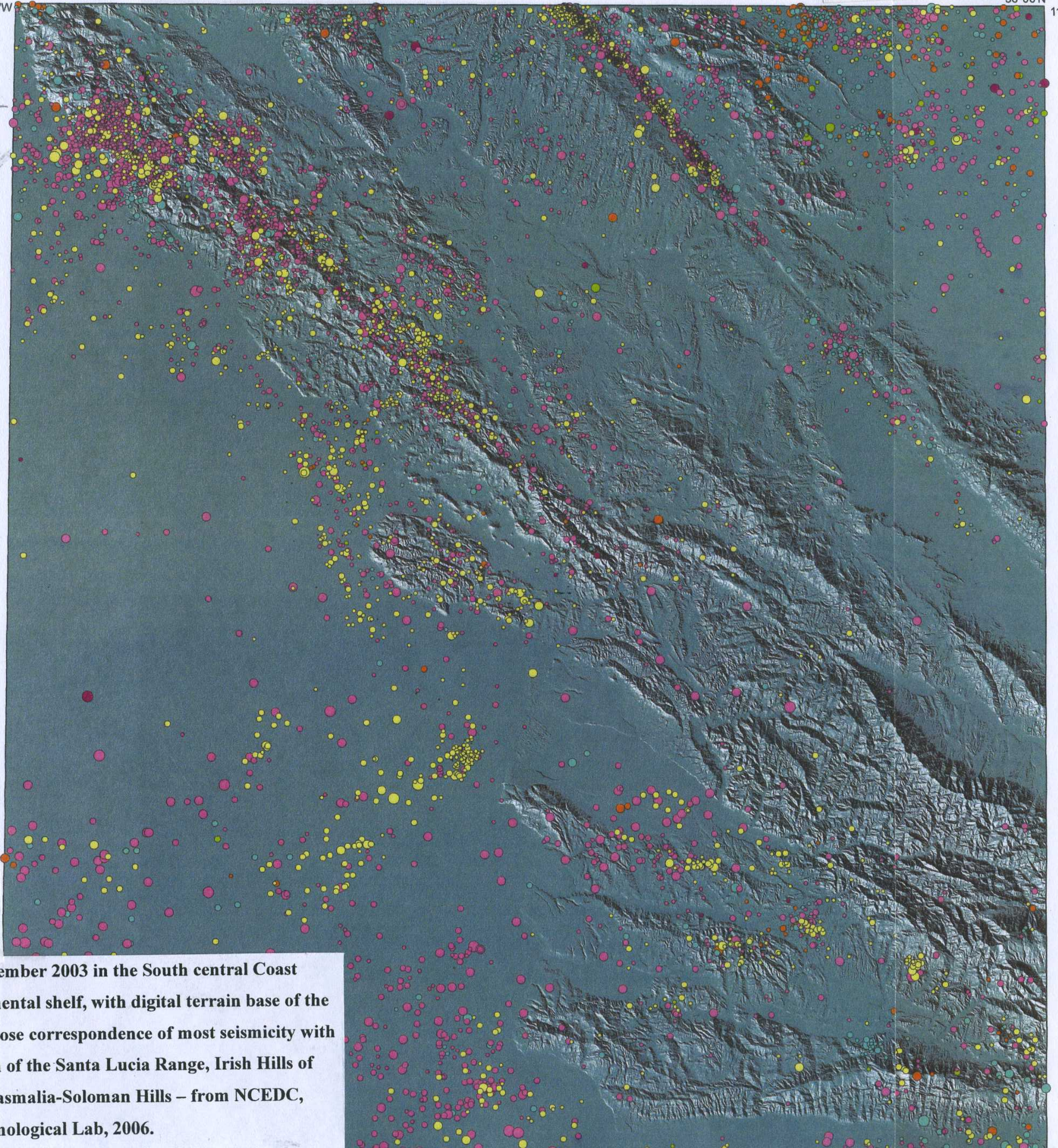

Seismicity prior to late December 2003 in the South central Coast Ranges and adjacent continental shelf, with digital terrain base of the onshore region. Note the close correspondence of most seismicity with the uplifted tectonic terrain of the Santa Lucia Range, Irish Hills of the San Luis Range, and Casmalia-Soloman Hills – from NCEDC, 2006, plotted by UNR Seismological Lab, 2006.

Figure 8

Earthquake focal mechanisms, southern Coast Ranges, western Transverse Ranges and adjacent offshore region, from McLaren et al., 2008 and Hardebeck, 2010

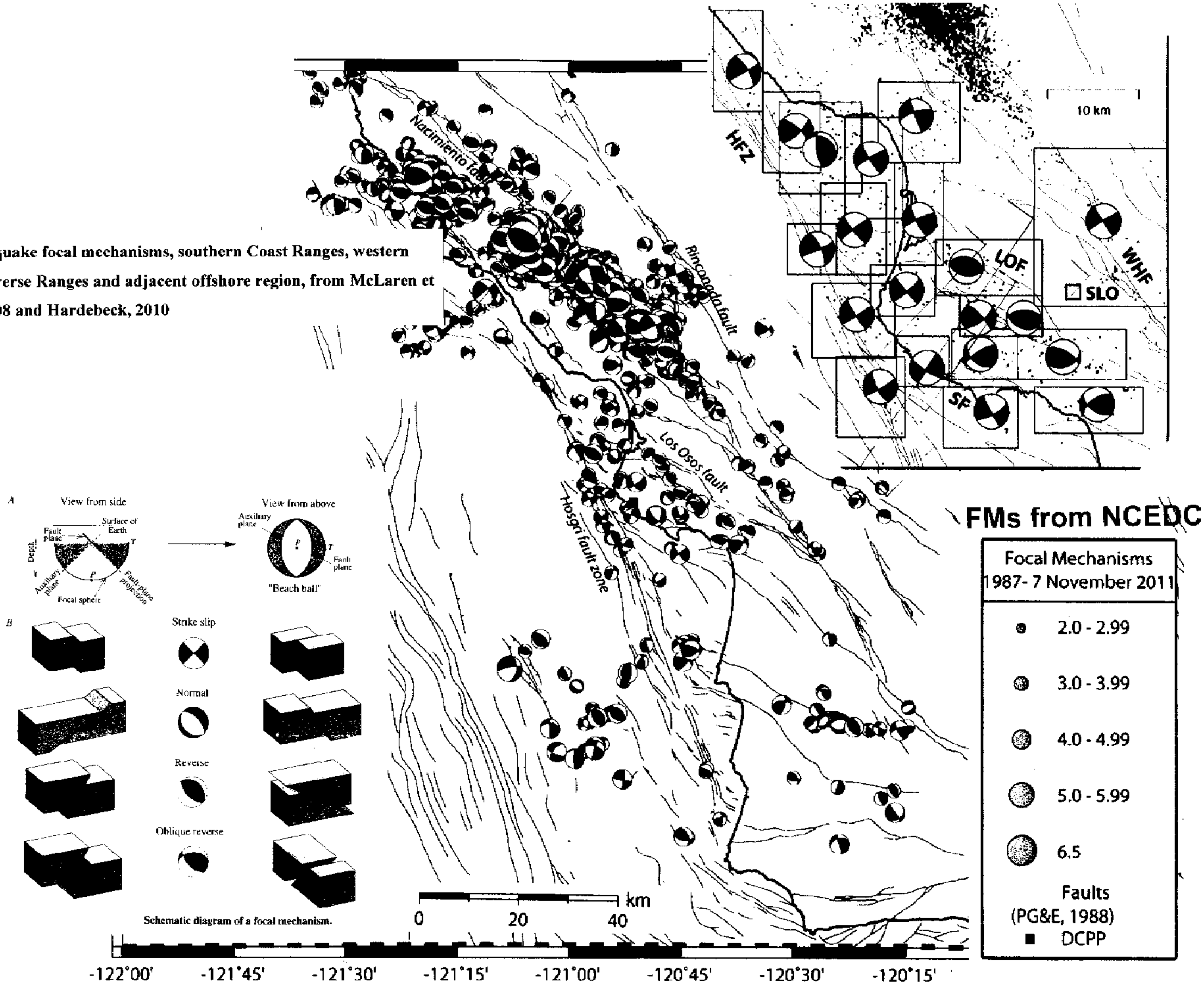

Schematic diagram of a focal mechanism.

Figure 9

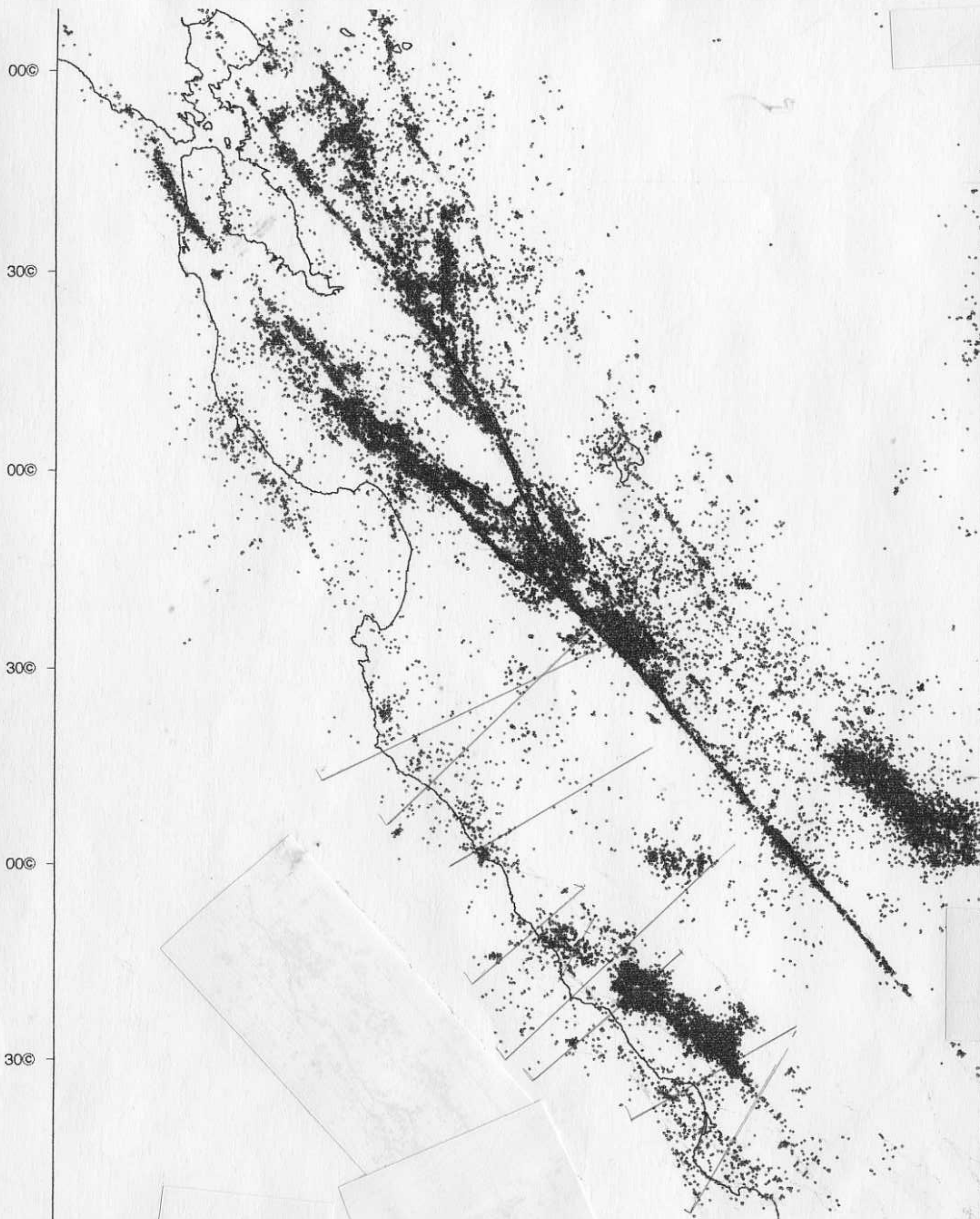

Seismicity in the central and southern Coast Ranges and adjacent offshore, recorded since 1980 based on relocations by Waldhauser and Schaff (2008) north of 36°N. Inset plot shows seismicity in the south-central Santa Lucia Range through early December 2003, prior to the 2003 M6.5 San Simeon earthquake. Locations of seismicity hypocenter cross sections are shown on this plot and are identified as to section designation on Figure 10b

Figure 10a

Digital terrain image of the central and southern Coast Ranges and western extent of the western Transverse Ranges. The traces of offshore reaches of the San Gregorio Hosgri fault zone are based on seismic reflection geophysical data. The trace of the offshore Shoreline fault is based on the alignment of small earthquakes along it and south of Point Buchon, on its sea floor terrain expression as seen on Multibeam sea floor imagery. Locations of seismicity cross sections and Google earth oblique aerial views of tectonic terrain features are plotted

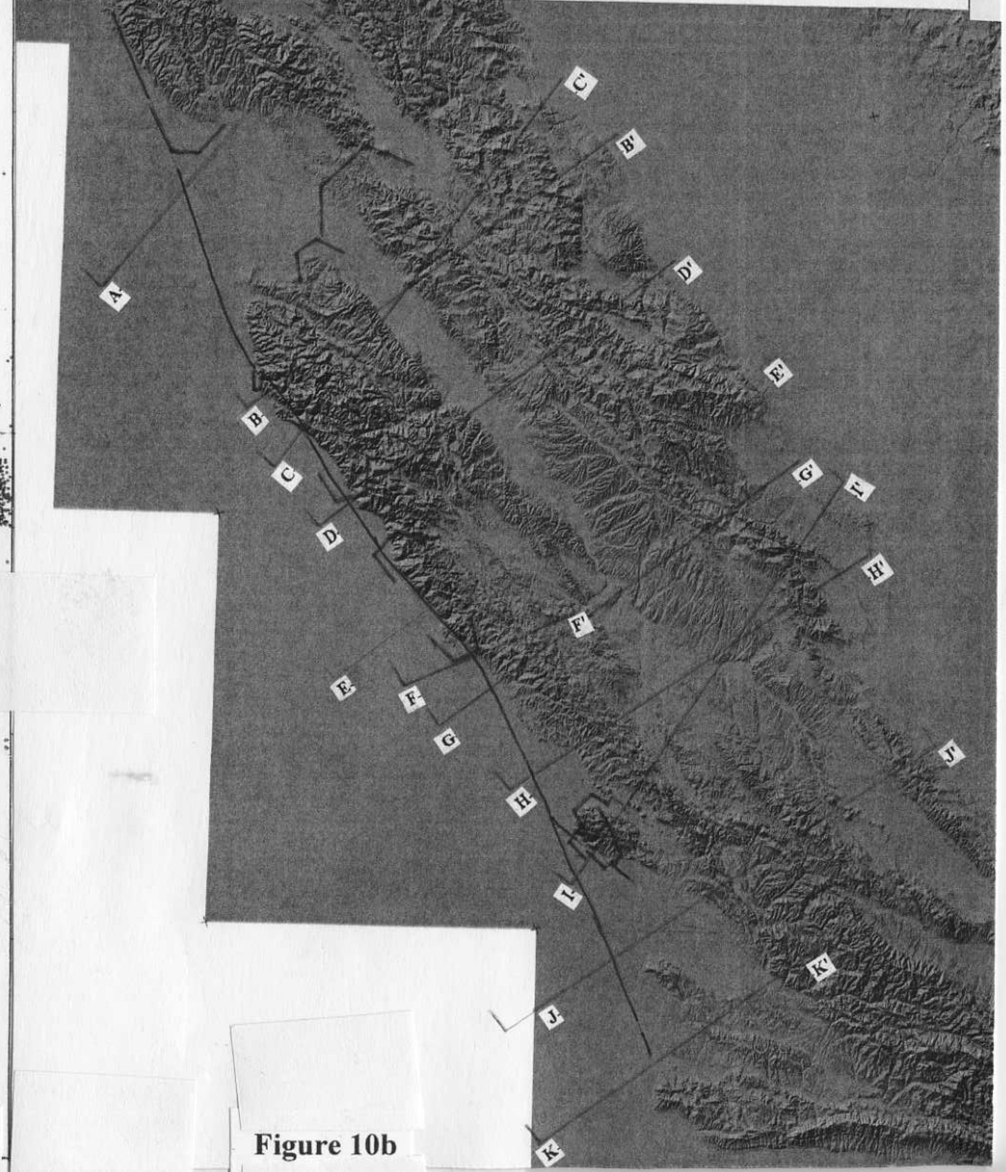

Figure 10b

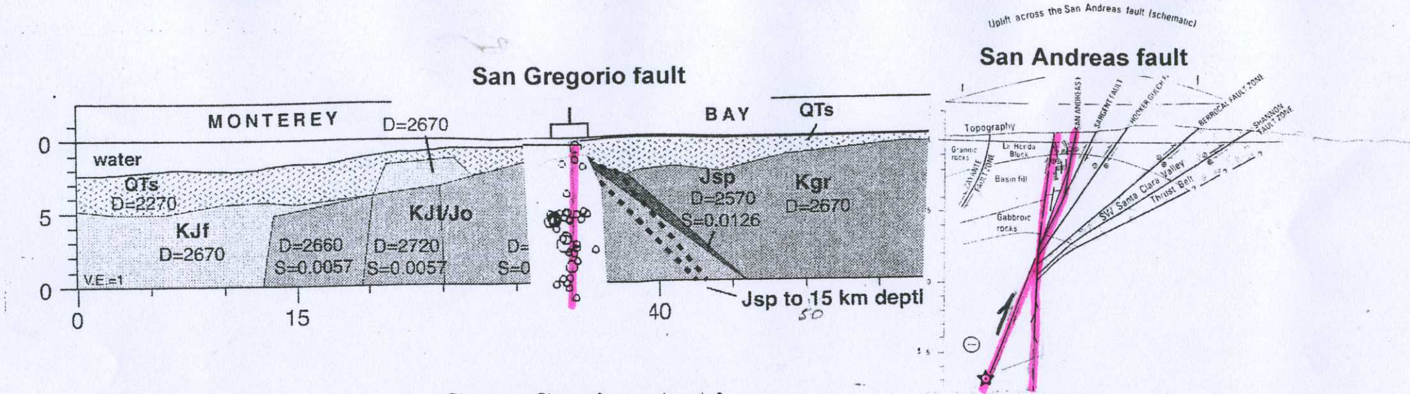

Cross Section A-A'

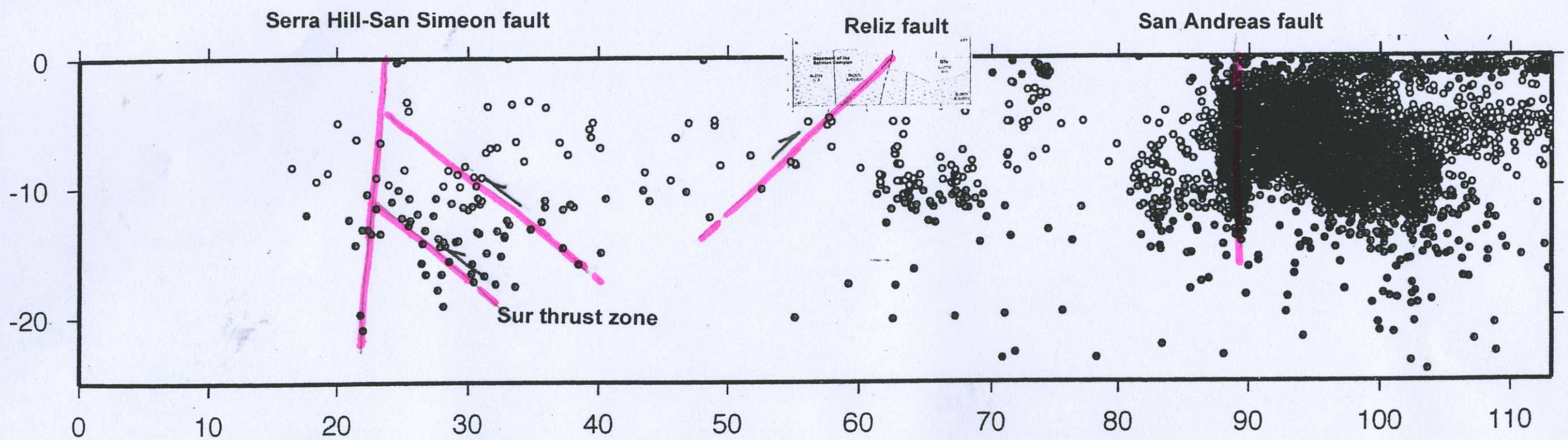

Cross Section B-B'

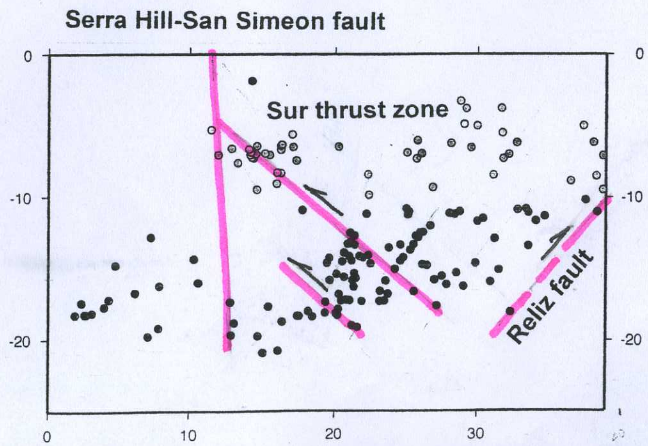

Cross Section C-C'

Figure 11

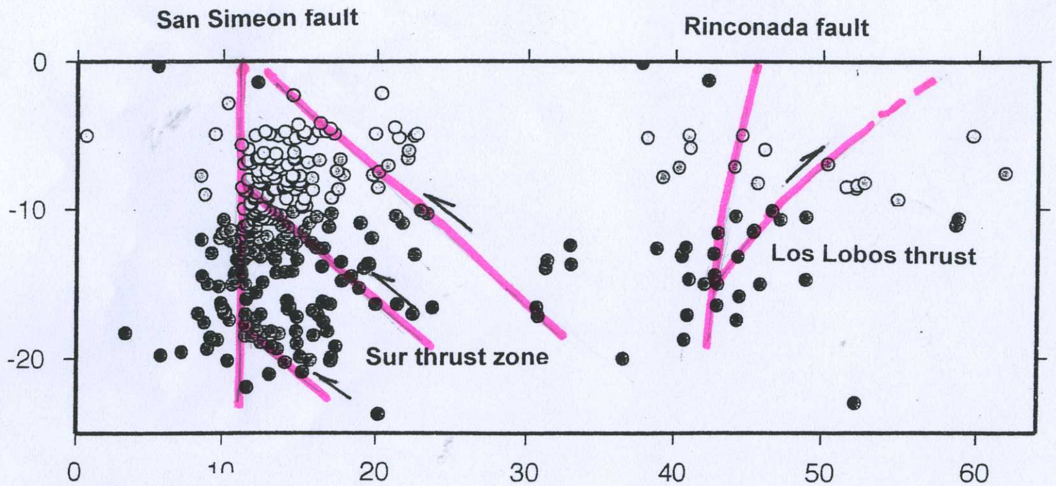

Cross Section D-D'

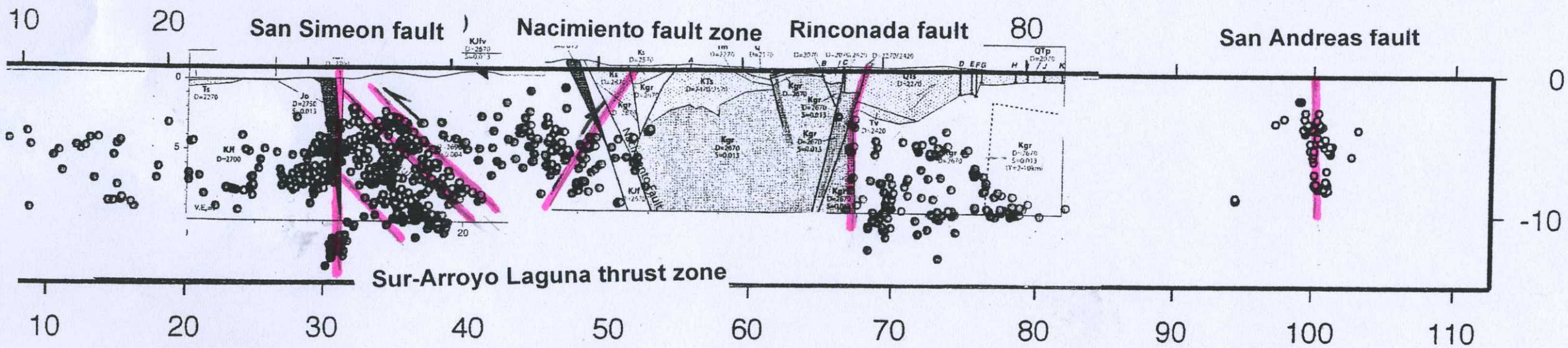

Cross Section E-E'

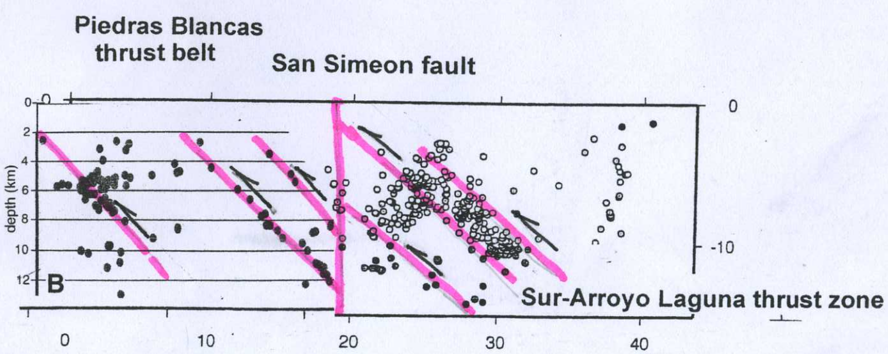

Cross Section F-F'

Figure 12

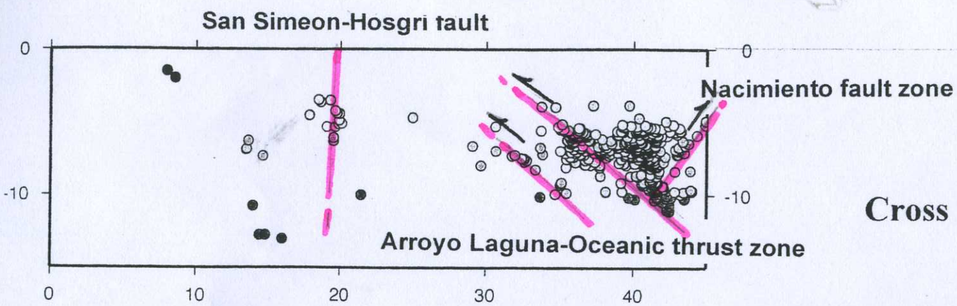

Cross Section G-G'

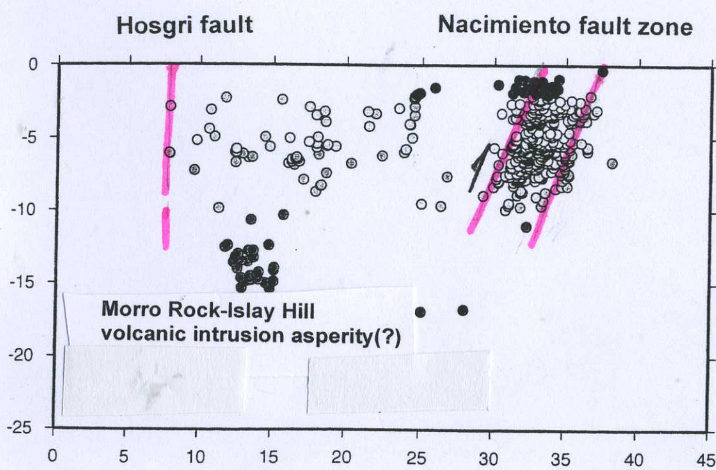

Cross Section H-H'

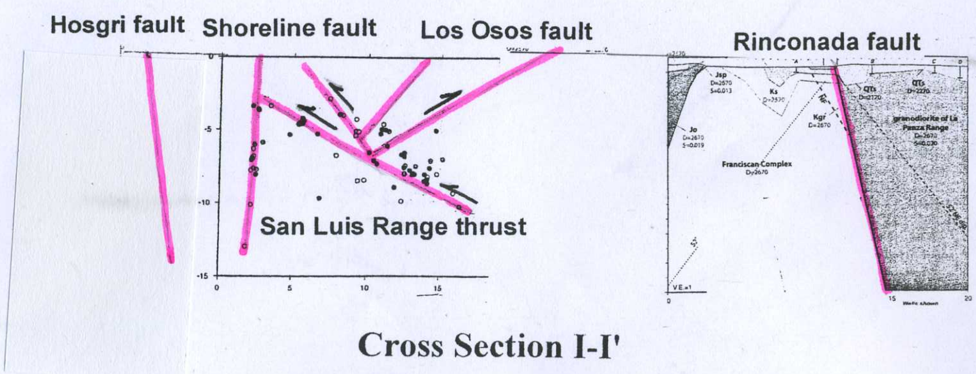

Cross Section I-I'

Figure 13

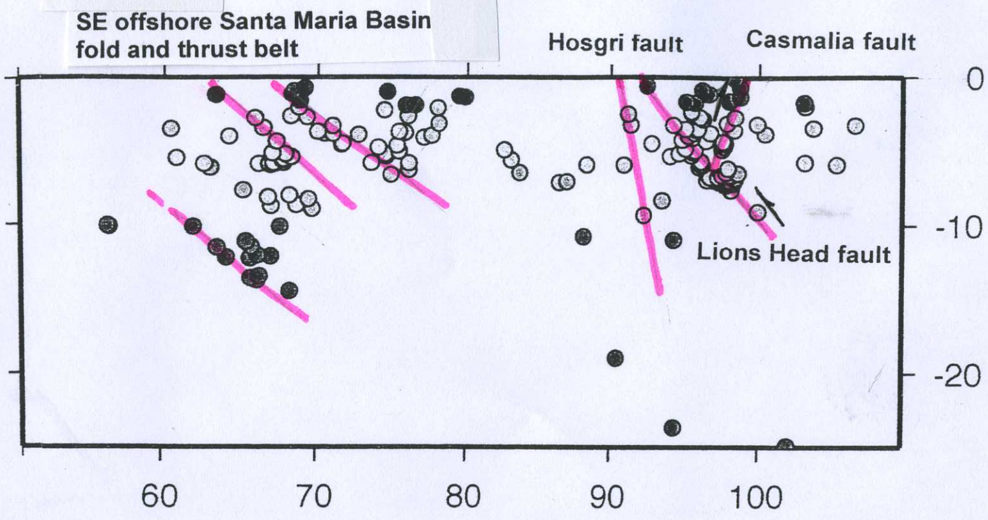

Cross Section J-J'

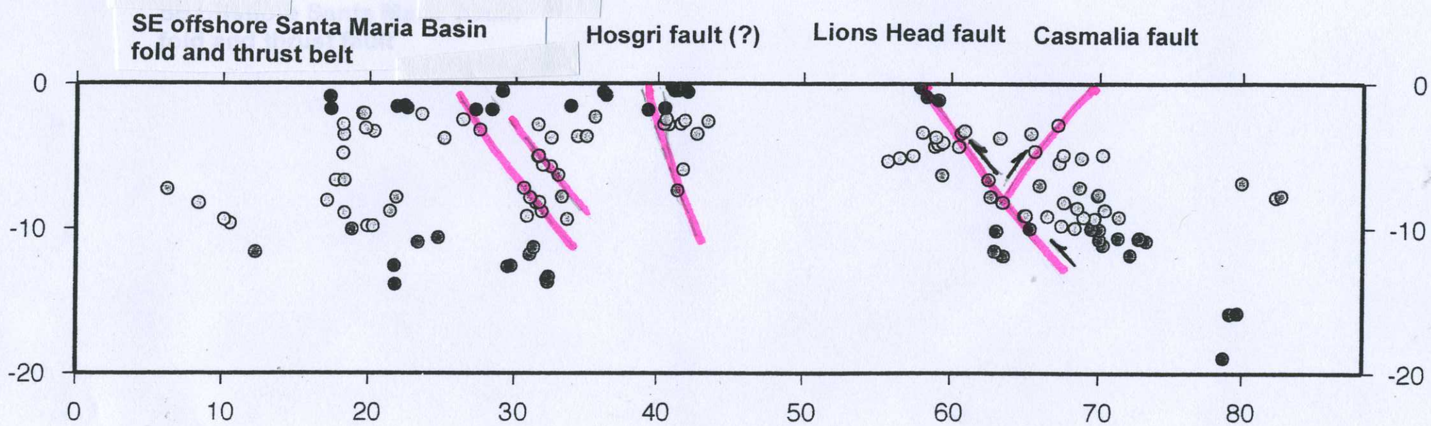

Cross Section K-K'

Figure 14

View north of Santa Cruz Mountain Range domal uplift welt along the west side of the San Andreas fault

Figure 15

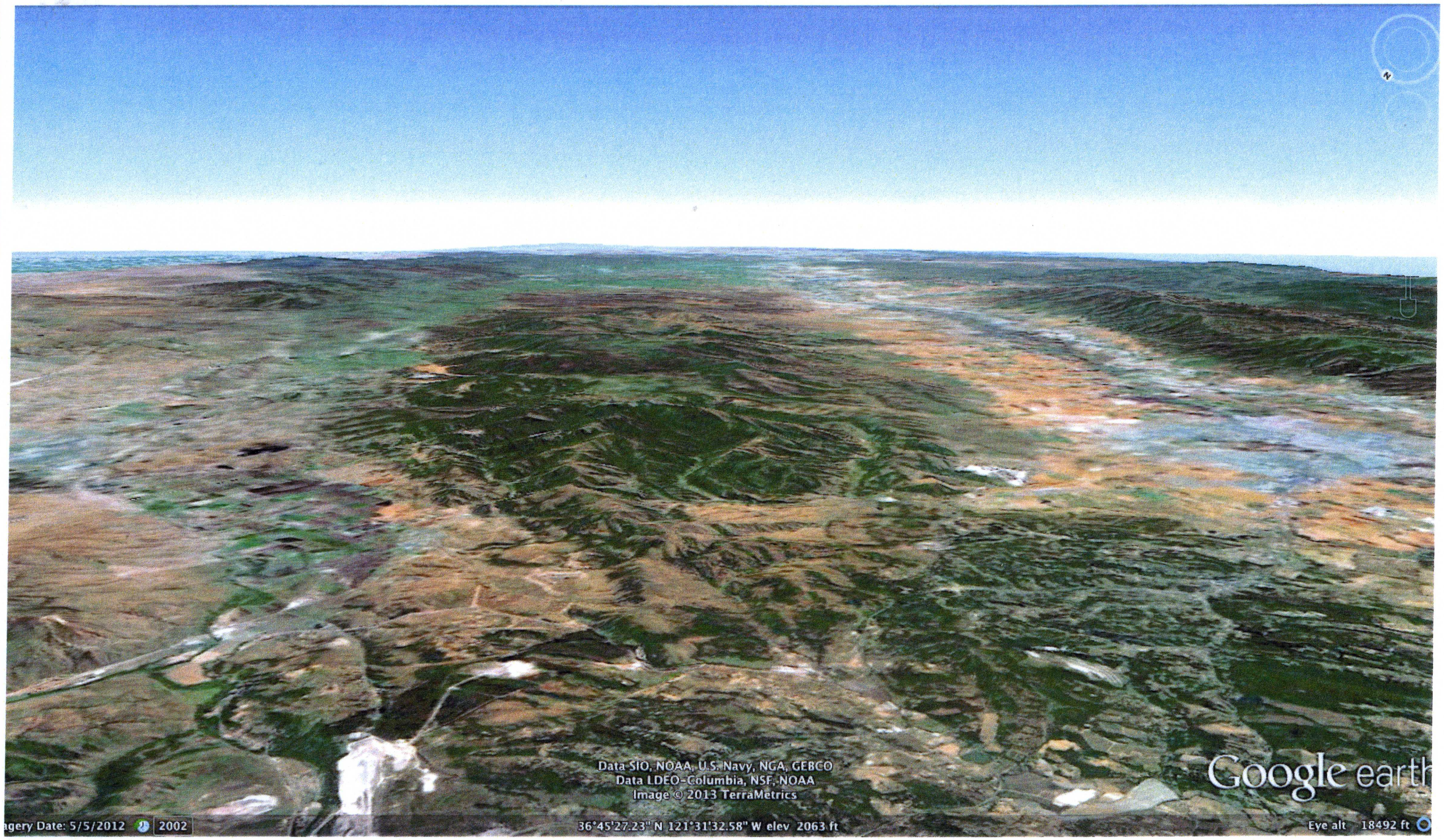

View south showing Gabilan Range uplift welt along the west side of the San Andreas fault, which extends across the lower left quadrant of the image. The Reliz fault east frontal scarp of the northern Santa Lucia Range is visible in the upper right quadrant of the image.

Figure 16

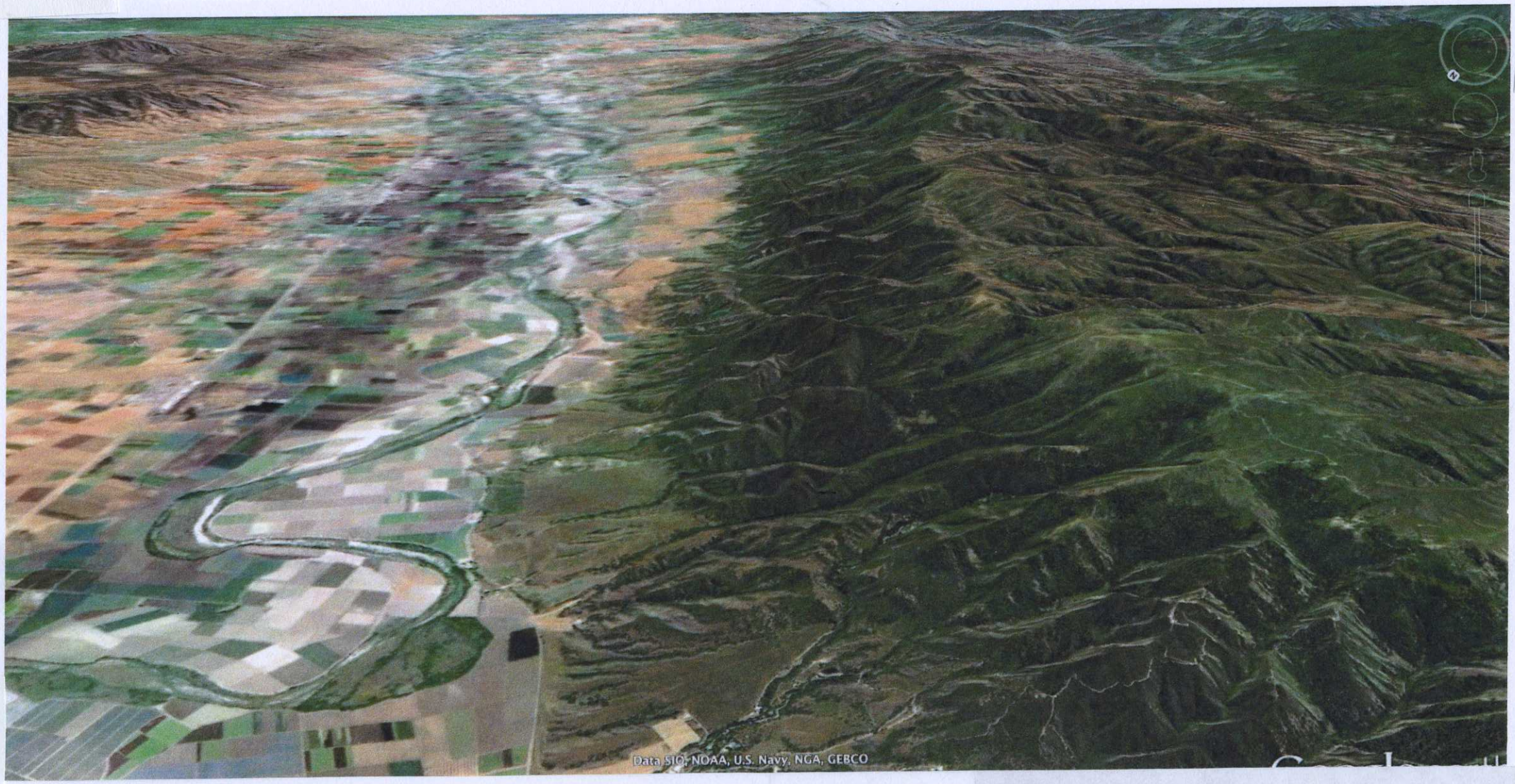

View south showing Salinas Valley and Sierra de Salinas Reliz fault east frontal scarp of the northern Santa Lucia Range wedge-block uplift (Seismicity Cross Section B-B').

Figure 17

Terrace-level view of the Sur fault-line escarpment terrain north of Soberanes Point, northern Santa Lucia Range.

Figure 18

View north along the west facing range-front wedge-block uplift of the northern Santa Lucia Range along the concealed Sur fault. The distant Big Sur area of local uplift of the footwall side of the Sur fault, separated from the main range front across the Serra Hill fault reach of the San Gregorio-Hosgri fault zone, is seen in the upper left quadrant of the image.

Figure 19

View north of the coast line between Piedras Blancas Point at bottom and Point Sur in upper left. Uplift of the Santa Lucia Range wedge-block diverges eastward from the onshore San Simeon fault reach of the San Gregorio-Hosgri fault zone southward from Ragged Point in the lower right center of the image. This is an area of elevated seismicity down dip on the Arroyo Laguna reach of the Sur-Arroyo Laguna-Oceanic reverse fault zone.

Figure 20

View south from the vicinity of Cape San Martin showing the steep west-facing fault-line scarp range-front truncation of the uplifted central Santa Lucia Range wedge-block. The M6.5 2003 San Simeon earthquake occurred within the reverse faulting complex beneath the south-central Santa Lucia Range in the upper right quadrant of the image. The local offshore trace of the San Simeon reach of the San Gregorio-Hosgri fault extends on-land north of Ragged Point in the upper right quadrant of the image.

Figure 21

View south showing the east-facing scarp of the Los Osos fault along the east margin of the Irish Hills pop-up wedge uplift. The range front is being thrust over the adjacent Los Osos Valley along this late Quaternary fault.

Figure 22

View north along the canyon of Coon Creek in the northern Irish Hills. Rapid late Quaternary uplift of the Irish Hills pop-up wedge is indicated by the V-shaped incision of Coon Creek into an older broad-valley terrain.

Figure 23

View north from the vicinity of Point San Luis along the southwest-facing seaward flank of the Irish Hills. Uplift of the hills pop-up wedge occurs by upward movement of the wedge along the underlying San Luis Range thrust. In this area the northeast-dipping thrust intersects the vertical plane of the strike slip Shoreline fault in the subsurface.

Figure 24

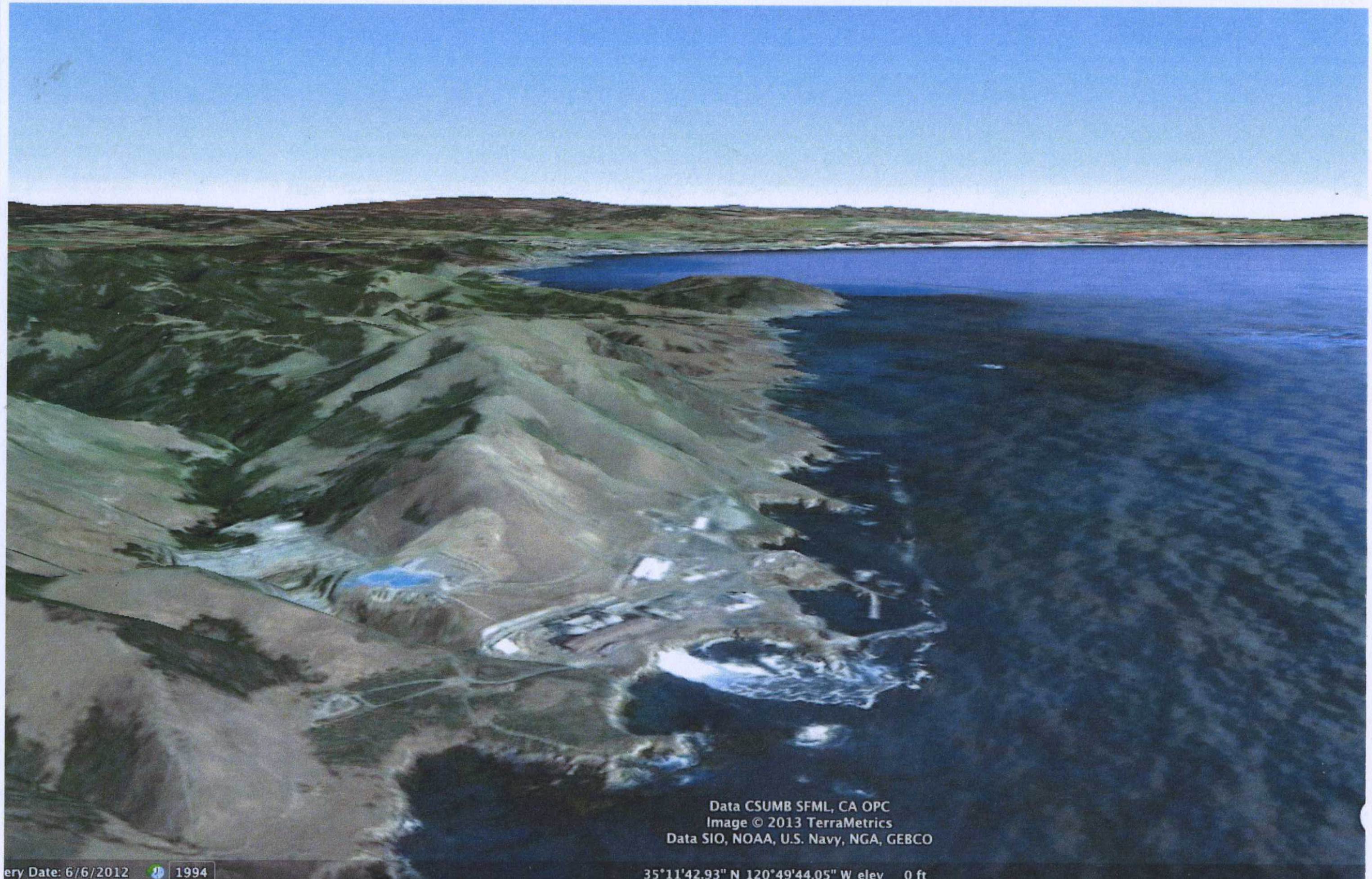

View southeast along the southwest coast of the Irish Hills, with Point San Luis in the upper right quadrant of the image. The Shoreline offshore fault parallels this coastline, hills are uplifting along the underlying northeast-dipping San Luis Range thrust, which intersects the vertical plane of the Shoreline fault at depth. Known onshore and offshore trace of the Diablo Cove reverse right oblique fault is in the lower right quadrant of image.

Figure 25

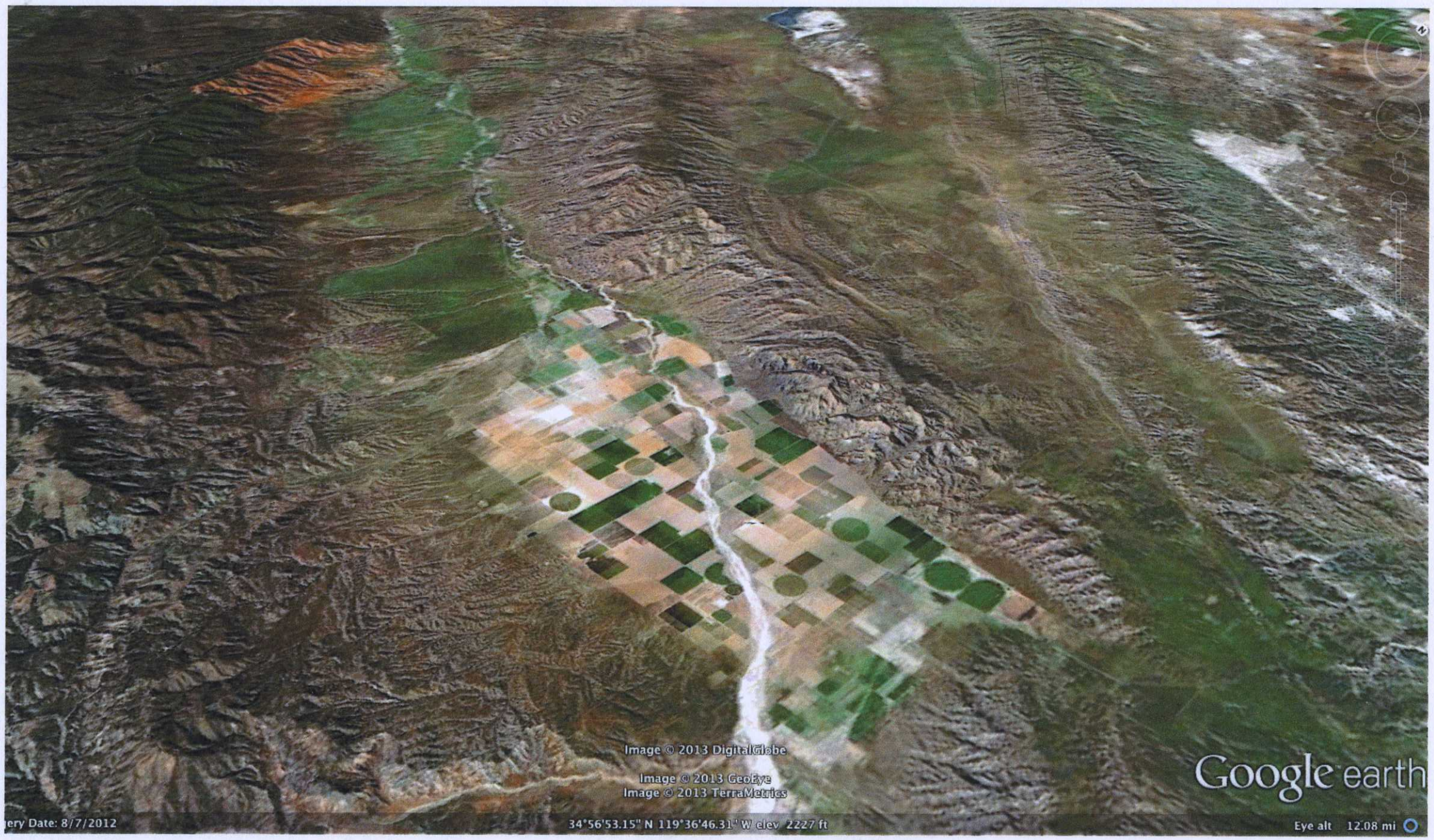

View northwest showing southwest-facing eroded frontal scrap of Morales fault in image center; San Andreas fault trace is seen in right quadrant.

Figure 26

Proposed kinematic neotectonic model, central and southern Coast Ranges, western Transverse Ranges, and southwestern Basin and Ranges.

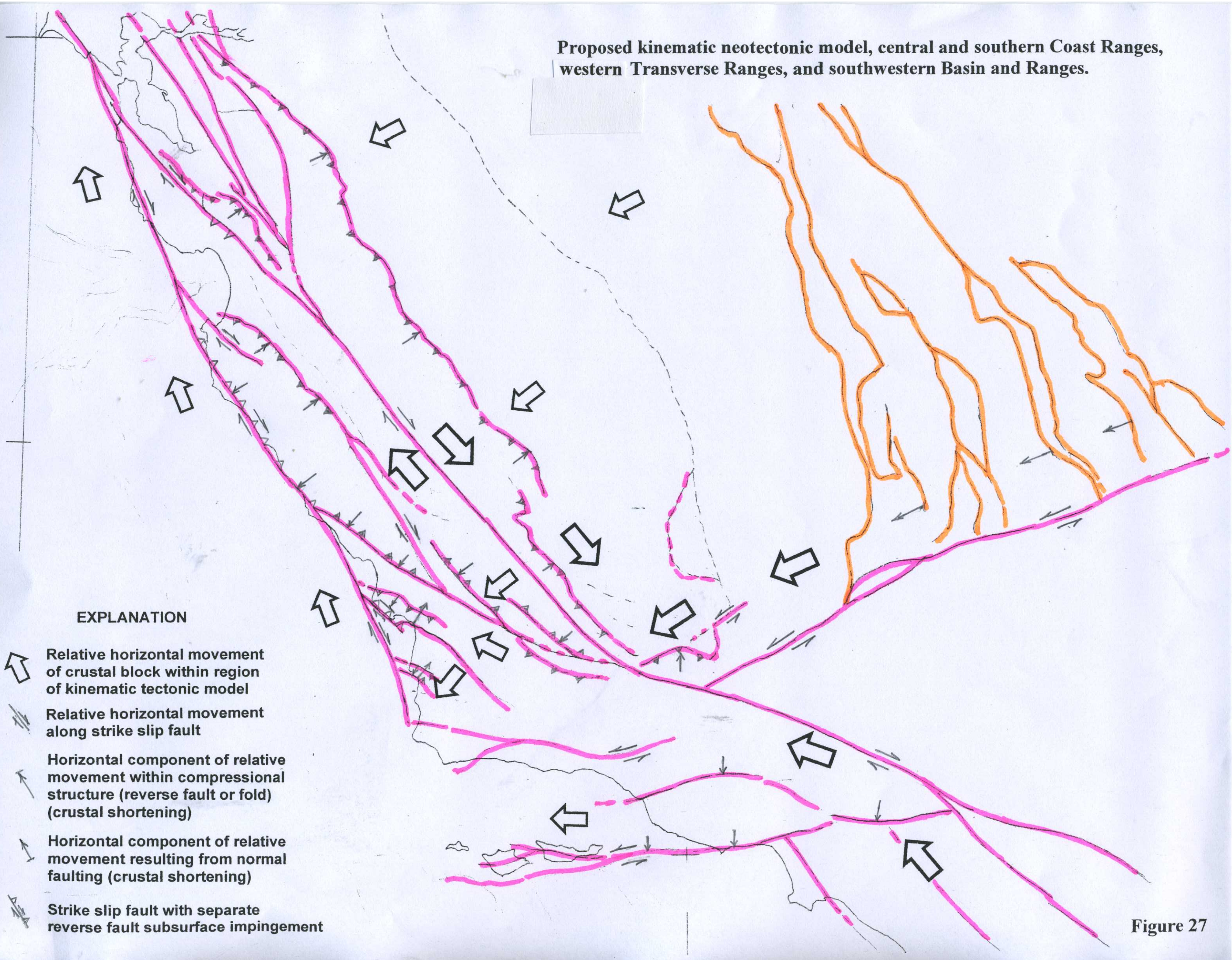

Figure 27